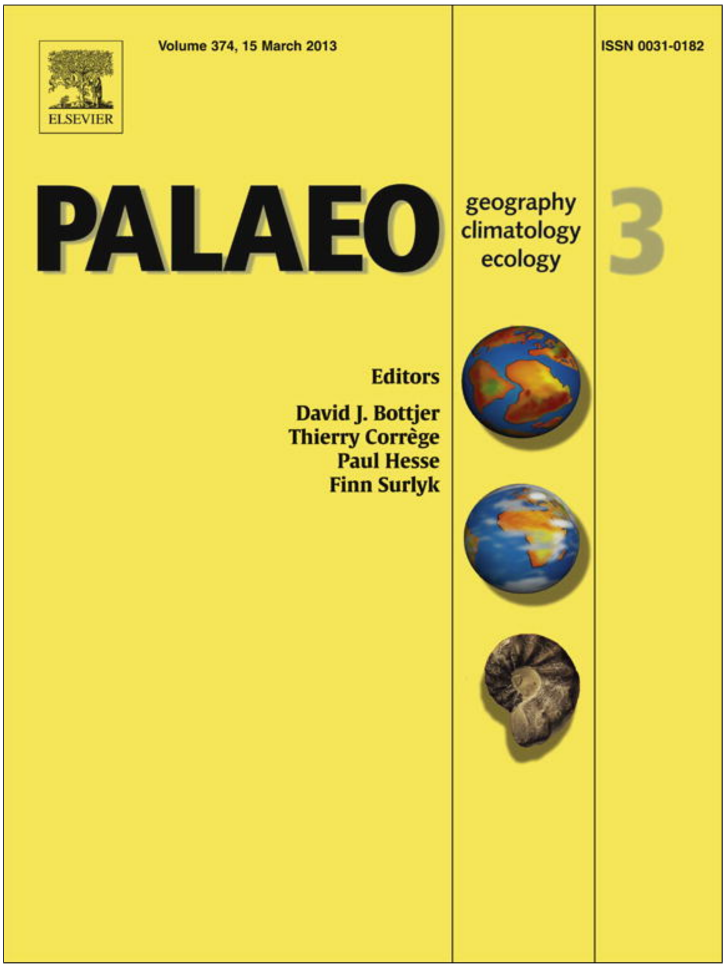
Volume 374, 15 March 2013
ISSN 0031-0182
ELSEVIER
PALAEO
geography
climatology
ecology
3
Editors
David J. Bottjer
Thierry Corrège
Paul Hesse
Finn Surlyk

Palaeogeography, Palaeoclimatology, Palaeoecology 374 (2013) 81–95

Contents lists available at SciVerse ScienceDirect

Palaeogeography, Palaeoclimatology, Palaeoecology

journal homepage: www.elsevier.com/locate/palaeo

Mio-Pleistocene Zanda Basin biostratigraphy and geochronology, pre-Ice Age fauna, and mammalian evolution in western Himalaya

Xiaoming Wang [a,b,e,*], Qiang Li [b], Guangpu Xie [c], Joel E. Saylor [d], Zhijie J. Tseng [a,e], Gary T. Takeuchi [f], Tao Deng [b], Yang Wang [g], Sukuan Hou [b], Juan Liu [b,h], Chunfu Zhang [i], Ning Wang [b], Feixiang Wu [b]

[a] Department of Vertebrate Paleontology, Natural History Museum of Los Angeles County, 900 Exposition Blvd., Los Angeles, CA 90007, USA
[b] Key Laboratory of Evolutionary Systematics of Vertebrates, Institute of Vertebrate Paleontology and Paleoanthropology, Chinese Academy of Sciences, Beijing 100044, PR China
[c] Gansu Provincial Museum, Lanzhou 730050, PR China
[d] Geology Program, School of Earth Sciences and Environmental Sustainability, Northern Arizona University, Flagstaff, AZ 86011, USA
[e] Integrative and Evolutionary Biology Program, Department of Biological Sciences, University of Southern California, Los Angeles, CA 90089, USA
[f] The George C. Page Museum of La Brea Discoveries, 5801 Wilshire Blvd., Los Angeles, CA 90036, USA
[g] Department of Earth, Ocean and Atmospheric Science, Florida State University, Tallahassee, FL 32306, USA
[h] Department of Biological Sciences, University of Alberta, Edmonton, Alberta, Canada, T6G 2E9
[i] Department of Geosciences, Fort Hays State University, Hays, KS 67601, USA

ARTICLE INFO

Article history:
Received 7 December 2012
Received in revised form 5 January 2013
Accepted 9 January 2013
Available online 18 January 2013

Keywords:
Tibetan Plateau
Zanda Basin
Miocene–Pliocene–Pleistocene
Fossil mammals
Stratigraphy

ABSTRACT

The Pliocene (5.3–2.6 Ma) of Tibet witnessed the drying of the northern Tibetan Plateau and the approach to the Pleistocene Ice Age within the background of intensifying Indian and East Asian monsoons. Yet little is known about Pliocene mammals living on the high Tibetan Plateau despite the fact that fossil mammals elsewhere constitute an important knowledge base for terrestrial environments. The late Miocene to Pleistocene Zanda Basin at the northern foothills of the Himalayas affords a welcome opportunity to evaluate the biological response to environmental change at high elevations. Abundant, well-preserved fossil mammals and fish from an 800-m continuous section of fine- to coarse-grained sediments thus open a rare window into a past biological world. For example, the discovery of an ancestral wooly rhino from Zanda Basin that was the precursor of its late Pleistocene megafaunal descendants leads to our "out-of Tibet" hypothesis, suggesting that the high Tibetan Plateau was a Pliocene cradle for Ice Age cold adaptations.

In this paper, we document in detail the mammalian biostratigraphy, chronology, and paleozoogeography based on Zanda Basin fossil mammals. Our high-resolution biostratigraphy and biochronology offer for the first time independent constraints that both support and modify recent magnetostratigraphic correlations. Using characteristic Pliocene and Pleistocene mammals, particularly the small mammal assemblages in the lower part of the section and monodactylid *Equus* from the upper section, we propose a correlation to C1n to C3An.1r, with an age range of ~400 Ka to 6.4 Ma.

Within the 800-m Zanda section, the lower 0–150 m is of latest Miocene age, spanning 6.4–5.3 Ma. Sparsely fossiliferous, the lower section has produced five taxa so far: *Ochotona*, *Panthera*, *Qurliqnoria*, *Palaeotragus*, and *Hipparion*—all are consistent with a late Miocene age. The middle 150–620 m section spans the entire Pliocene. This section is by far the most fossiliferous, including such typical Pliocene small mammals as *Prosiphneus*, *Mimomys*, *Apodemus*, and *Trischizolagus*, as well as large mammals such as *Coelodonta thibetana*, *Hipparion zandaense*, *Chasmaporthetes*, *Nyctereutes*, *Meles*, *Antilospira*, and others. In the upper 620–800 m section the fossils are rare, but do include characteristic Pleistocene taxa such as *Equus*.

Zoogeographically Zanda Basin mammals are a mixture from two major sources. Taxa such as *Mimomys*, *Prosiphneus*, *Trischizolagus*, *Chasmaporthetes*, *Nyctereutes*, *Meles*, and *Xenocyon* are commonly found in north China or east Asia. In contrast, several forms, such as unique species of pikas (*Ochotona*), squirrels (*Aepyosciurus*), and ancestral Tibetan antelope (*Qurliqnoria*), seem to belong to an indigenous Tibetan fauna evolved within the plateau. A lack of shared taxa with the Oriental Realm suggests a formidable barrier by the Himalayas despite a short distance (~100 km) between Zanda Basin and the Indian subcontinent.

1. Introduction

The Tibetan Plateau has been widely recognized as central to our understanding of the evolution of the Indian and Eastern Asian monsoon

* Corresponding author at: Department of Vertebrate Paleontology, Natural History Museum of Los Angeles County, 900 Exposition Blvd., Los Angeles, CA 90007, USA. Tel.: +1 2137633310; fax: +1 2137467431.
E-mail address: xwang@nhm.org (X. Wang).

0031-0182/$ – see front matter
http://dx.doi.org/10.1016/j.palaeo.2013.01.007

systems, and debates are on-going about the timing of uplift process and its role in initiating changes in climatic regime (e.g., An et al., 2001; Molnar, 2005; Boos and Kuang, 2010; Quade et al., 2011). Until fairly recently direct evidence of the effect of this changing regime on the biological community, especially vertebrates, has been sparse and has played a limited role in the debate (e.g., Ji et al., 1980; Huang and Ji, 1981). To a large extent, this is the result of the recent start of paleontological research efforts and a lack of suitable basins with abundant fossils. Added to this are difficulties in physical access to mountainous terrains and political sensitivity.

Zanda (Zhada) Basin offers an exceptional opportunity to remedy this shortcoming and to begin building an excellent fossil record to test relationships of paleoenvironments and vertebrate evolution in a crucial region of the Tibetan Plateau. The basin's location in the northern foothills of the western Himalaya, at high elevations, and at the headwaters of the Indus River contributes to a unique perspective in the paleozoogeography of its ancient faunas. Nearly four months of field work over five seasons (2006–07, 2009–10, 2012) demonstrate that this is the richest basin on the Tibetan Plateau in terms of abundance of fossil material, areas of potential exposures, and continuity of the fossil record. Archived in well-preserved and extensively exposed late Miocene to Pleistocene sediments, the Zanda fossil assemblage fill a critical void in the late Cenozoic, augmenting heretofore limited knowledge of Pliocene vertebrate faunas in southern Tibet and providing a much needed window into the past paleoenvironment and its effect on biological evolution.

Vertebrate paleontology in Zanda Basin significantly advances our understanding of the following aspects of the history of Tibet: 1, vertebrate communities and diversity in the late Cenozoic; 2, mammalian biochronology and magnetostratigraphy; 3, zoogeographic origins of individual components in Tibetan Plateau faunas; 4, paleoclimate records as preserved in isotopes of vertebrate teeth and bones; 5, paleoenvironments and plant communities as related to the diet of mammalian herbivores; 6, evolution of community structures in mammals and fishes; 7, relationship of cold adaptation in high elevations and for Ice Age megafaunas; and 8, drainage evolution of the Indus River system.

Our discovery of an ancestral wooly rhino from Zanda Basin made the unexpected link to its Ice Age descendants in northern Eurasia, establishing Tibet as a possible cradle of evolution for the Ice Age megafauna (Deng et al., 2011). The implications of this discovery highlight the importance of understanding major players in the vertebrate faunas and paleoenvironmental conditions during the Pliocene of Tibet, prior to the Ice Age. In this paper, we document in detail the biostratigraphic basis of our “out of Tibet” hypothesis. Our high resolution biostratigraphy lays the foundation for a chronologic framework, on which subsequent descriptions of individual taxa can be built, and will serve as an important reference point in the late Miocene to Pleistocene of Tibet.

2. Material and methods

All vertebrate fossils collected belong to and are housed in the Institute of Vertebrate Paleontology and Paleoanthropology (IVPP), Chinese Academy of Sciences. All Zanda fossil localities begin with an abbreviation of “ZD” followed by the last two digits of the year collected and the field number of that year, such as IVPP locality ZD0604 (04 locality in 2006). For east Asian biochronology, we use the latest proposal of the Chinese land mammal age/stage system by Qiu et al. (in press-b). We adopt the ATNTS2004 Geomagnetic Polarity Time Scale (GPTS) of Lourens et al. (2004) in our magnetic correlations. We define the Pliocene–Pleistocene (Neogene–Quaternary) boundary at C2r–C2An (2.581 Ma), as was recently endorsed by the International Commission on Stratigraphy (Mascarelli, 2009).

We devised a system of using elevation data to correlate individual localities with a master magnetic section in south Zanda. We systematically took GPS readings for all fossil localities, in many cases using the averaging function to achieve greater accuracy. The elevation data are interpolated into individual legs of the nearest measured sections by Saylor and colleagues (Saylor, 2008; Saylor et al., 2010b). We then adopted the lithostratigraphic and sequence stratigraphic correlation scheme by Saylor et al. (2010b) to tie together individual sections to a standard south Zanda magnetic section. The greatest advantage of such a system is that it permits us to closely tie all of our localities with six major measured sections, plus six other smaller partial sections. In most cases, the measured sections are in the same accessible canyons where fossils were collected, and distances of fossil localities to section legs are as small as a few hundred meters to as large as a few km. Because the basin is undeformed and bedding is horizontal, this method of lateral interpolation permits reasonable precision. The biggest source of systemic errors is probably GPS accuracy. In mountainous terranes, such as Zanda Basin, horizontal errors of 6–10 m or less by commercial grade GPS units can be routinely achieved, but errors of vertical measurements can be twice as much, or more. Such systemic errors can translate to an error in age estimates of ± 0.2 million years (assuming a 1 m/10,000 year sedimentation rate), a tolerable range given the common rate of mammalian speciation of greater than 1 myr (Blois and Hadly, 2009; Uyeda et al., 2011). Our calibration system can be improved by future magnetic studies on individual canyons, in combination with our locality database.

3. Previous paleontologic studies

Physical inaccessibility, political barriers, and the lack of a “dragon bone” hunting tradition by native Tibetans combined to make Zanda Basin practically unknown paleontologically until quite recently, despite the fact that the basin is one of the richest in vertebrate fossils on the Tibetan Plateau. Hints of the existence of fossil mammals first came to the fore in a report on a maxillary of an extinct giraffe *Palaeotragus* collected from Xiangze Farm area (now Jiade Farm) in 1976 by a group of geologists from a multidisciplinary Qinghai–Tibetan Plateau expedition by the Chinese Academy of Sciences (Zhang et al., 1981). News of vertebrate fossils inspired another geologist, Liang Dingyi, to make a trip himself in 1982, which led to the acquisition of a partial skull and jaws of a three-toed horse near the village of Daba. This specimen was later described as a new species *Hipparion zandaense* by Li and Li (1990). In the early 2000s, another team of geologists from the Institute of Geomechanics (Chinese Academy of Geological Sciences) made miscellaneous discoveries of a rhinoceros foot bone and a pika cheek tooth (Meng et al., 2004, 2005) that were too poorly preserved to be of significance.

All previous fossil discoveries were chance encounters of isolated specimens by geologists: our 2006 field season was the first documentation of the basin by vertebrate paleontologists. Our paleontologic explorations, spanning five field seasons (in 2006, 2007, 2009, 2010, 2012), thus represent the first systematic effort to assess the vertebrate fossil record in the basin. It soon became clear that Zanda Basin is ideally suited for paleontologic explorations: within our five short field seasons, several hundred specimens have been collected through much of the strata. However, only a new wooly rhinoceros and a partially preserved articulated skeleton of a three-toed horse have so far been adequately described (Deng et al., 2011, 2012), as well as a brief mention of the Zanda fauna in a summary paper on Tibet mammal biochronology (Wang et al., in press-a, in press-b). This report presents, for the first time, a detailed framework of biostratigraphy and geochronology, and full descriptions of individual taxa will follow in separate treatments.

Biostratigraphically, the lack of previous paleontologic explorations in Zanda Basin has a positive effect. Lacking historic “baggage” (such as in numerous Chinese basins with rich “dragon bone” hunting traditions, where fossils were acquired with questionable or no stratigraphic context) we are able to place every collected specimen in precise stratigraphic context. The only exceptions are two previously described specimens of *Palaeotragus microdon* (Zhang et al., 1981) and *Hipparion zandaense* (Li and Li, 1990) that lack detailed locality information. We are thus able to place all fossils in a modern stratigraphic context with a high resolution and consistency rarely seen in other Chinese basins.

4. Geologic and environmental setting

The Zanda Basin is a late Miocene through Pleistocene pull-apart sag basin located just north of the high Himalayan ridgecrest in the west-central part of the orogen (Fig. 1). Flanked by the Himalaya Range to the southwest and Ayilariju Mountain to the northeast, basin sediments can be seen as far southeast as 31°06′ N 80°35′ E near the village of Qulong in the upper reach of the Langqên Zangbo (Sutlej) River and as far northwest as the Qusong area; current outcrop extent of the basin fill is >9000 km^2.

The basin occupies a region with an extended tectonic history. To the northeast of the basin, the Oligo-Miocene Great Counter Thrust (GCT), a south-dipping, top-to-the-north thrust system, modifies the Indus Suture (e.g., Ganser, 1964; Yin et al., 1999; Murphy and Yin, 2003). The South Tibetan Detachment System (STDS), southwest of the basin, is an early-mid Miocene (Hodges et al., 1992, 1996; Searle et al., 1997; Murphy and Harrison, 1999; Hodges, 2000; Murphy and Yin, 2003; Searle et al., 2003; Yin, 2006; Cottle et al., 2007) series of north-dipping, low-angle, top-to-the-north normal faults. Zanda Basin sediments onlap, and hence post-date movement on, both the STDS and the GCT. Ongoing exhumation of the Gurla Mandhata metamorphic core complex to the southeast of the basin began at ~9 Ma (Murphy et al., 2002). Qusum (Leo Pargil) metamorphic core complex to the northwest basin began at 14–16 Ma (Thiede et al., 2006) and these faults cut Zanda Basin sediments (Saylor et al., 2010a). The axis of the basin is approximately northwest–southeast, parallel to the general arc of the Himalaya. Tectonic control, basin geometry, basin sedimentology, depositional environment, drainage evolution, stable isotopes, paleoclimates, and elevation history have been explored during the recent decade (Saylor, 2007; Saylor et al., 2007a, 2007b; Saylor, 2008; Saylor et al., 2008; Wang et al., 2008a, 2008b; Kempf et al., 2009; Saylor et al., 2009, 2010a, 2010b; Quade et al., 2011; Y. Wang et al., 2011, 2012).

With an elevation of 3700–4500 m, modern Zanda Basin has an annual mean temperature of close to 0 °C (based on data from nearby Shiquanhe in National Climatic Data Center, 2012). Located at the western end of the Himalaya and on its northern flank (~31–32° N, 79–80° E), this region has a relatively dry summer created by long distance from and degradation of the combined effects of Indian and Southeast Asian monsoons coming from the east and southeast (Böhner, 2006; Bolch et al., 2012), although summer rains account for ~80% of the annual precipitation in the area (Li, 2006; Tian et al., 2007). Winter, however, is relatively wet compared to eastern Himalaya because of the stronger influence of the winter Westerlies. If a similar monsoon system operated in western Himalaya during the Pliocene, then relatively heavier winter snow and a drier summer, compared to the eastern Himalaya, would be expected. Such a climatic regime seems to be a major factor on modern erosion, causing steeply incised canyons, and would have an impact on the evolution of pre-Ice Age Tibetan faunas.

5. Depositional setting and fossil preservation

Zanda Basin sediments show cyclical changes that may be attributed to Milankovitch forcing (Saylor et al., 2010b). The sedimentary basin fill is undisturbed and lies in angular or buttress unconformity with the underlying deformed Tethyan Sedimentary Sequence (TSS) strata. After deposition, incision by the Langqên Zangbo River exposed the entire basin fill. The basin fill consists of ~800 m of fluvial, lacustrine, eolian and alluvial fan deposits. The lower part of the section consists of ~200 m of trough cross-bedded sands and well-organized, imbricated, pebble to cobble conglomerate. Associated sedimentary structures include stacked, 3–4 m sand–gravel filled channels and longitudinal bars. We interpret these features as fluvial deposits laid down by large-scale rivers ancestral to the Sutlej or Indus based on provenance and

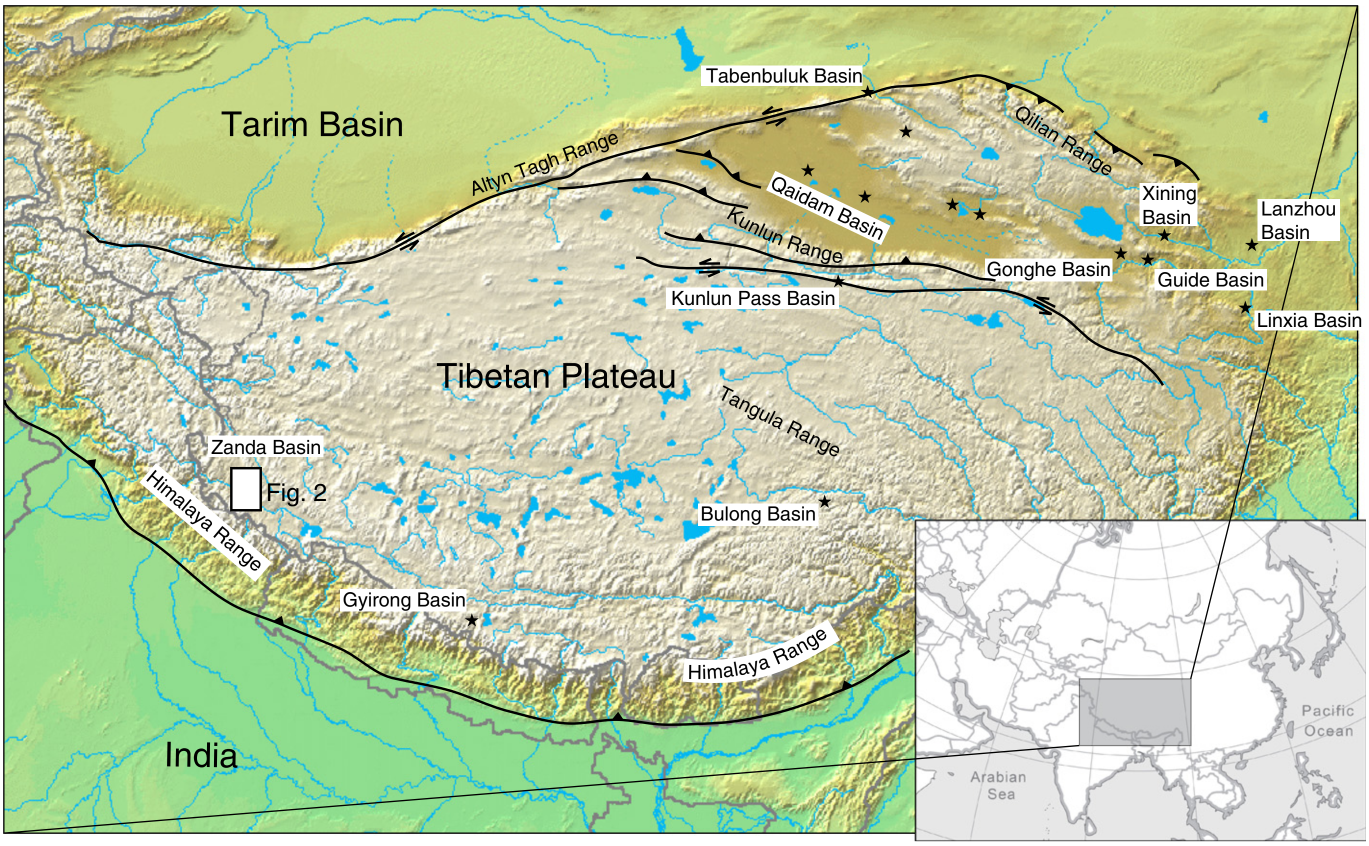

Fig. 1. Map of known basins producing fossil vertebrates in the Tibetan Plateau. Political boundaries in the maps do not imply any opinion concerning the legal status of any country or territory.

paleocurrent orientation data (Saylor et al., 2010a). Interbedded fine-grained sand and silt horizons showing extensive soft-sediment deformation and containing abundant mammal, gastropod and plant macrofossils are interpreted as marshy bog or overbank deposits within a low-gradient fluvial setting. The middle unit (approximately 250 m) consists of an upward coarsening succession of lacustrine progradational parasequences. Individual parasequences are up to 17 m thick and range between profundal lacustrine claystones and deltaic and wave-worked sediments, including evidence of occasional desiccation. The top 350 m continues the upward coarsening progression displayed in the middle portion but becomes much coarser. The profundal lacustrine facies disappears and is replaced by deltaic or lake-margin deposits. Individual parasequences vary between deltaic or lake-margin and alluvial-fan and fan-delta conglomerates.

Since the initial establishment of the Zanda Formation as a lithological unit (Zhang et al., 1981), additional formation (such as the Tuolin and Xiangze formations) or even group (Zanda Group) names were proposed (Zhu et al., 2005), often based on a perceived depositional hiatus that later proved to be false (Wang et al., 2008b; Saylor et al., 2009). Here we follow Saylor et al. (2009, 2010a, 2010b) and use a single unit, Zanda Formation, for the entire basin sequence.

Vertebrate fossils are present in most fine- to medium-grained sediments in most accessible exposures that are not too steeply incised (Fig. 2). Fossil fishes are found throughout the middle unit, particularly in fine-grained sediments (Figs. 3, 4). Fossil mammals, especially large mammals, are most abundant in near-shore facies and often closely associated with exposures of basement rocks, which often formed islands or the shore line of the Zanda paleo-lake (Fig. 2). We have systematically searched for fossils in all exposures that are approachable by off-road vehicles. Nonetheless our limited efforts were mostly concentrated in areas of high promise, based on satellite images, and are far from an exhaustive search.

The high-energy conglomerate units from the upper and lower portions of the Zanda Formation are mostly unfossiliferous except for a handful of Pleistocene localities producing large mammal fragments. Our prospecting was thus mainly focused in the median to fine-grained unit in the middle section. However, the very fine-grained 220–320 m section mainly produces fish (Fig. 4). With the exception of a partially articulated wooly rhinoceros skeleton from IVPP locality ZD1055 and occasional partial fish skeletons, the vast majority of mammal and fish fossils occur as single elements or a few associated bones or teeth. Partially articulated specimens are uncommon. In most cases the distance of transport is probably short. Concentrated fossil occurrences are exceedingly rare; we found only two sites (IVPP locality ZD1001 and ZD1208), by far our richest, in our five years of exploration that are worthy of extensive quarrying or dry-screening and IVPP locality ZD1001 has a concentration of both large and small mammals, apparently by a fluvial process.

6. Biostratigraphy and biochronology

Despite being in a tectonically active area, Zanda Basin strata underwent minimal post-depositional deformation. Bedding is flat-lying throughout most of the basin, and because of the dominance of shallow lake sediments, most bedding planes are perfectly horizontal and can be traced laterally for long distances. With deep incisions in the majority of exposures, visual correlation is possible in much of the basin. We took advantage of this unique preservation and devised a system of correlations using GPS elevations to tie all fossil localities to a master paleomagnetic section (see Section 2, Materials and methods).

However, such steeply incised canyons in the majority of exposures are not ideal for preservation and collection of fossils. Near-vertical cliffs not only are inaccessible for prospecting but also do not accumulate fossils when they are exposed and erode out. A total of 240 vertebrate fossil localities have been discovered during the past five seasons (Table 1). Of these, three are small mammal sites (IVPP localities ZD0609, 0904, 1001) yielding multiple taxa. Most of the rest of the localities are large mammals or fish bones, often yielding one or at most a few taxa. Preservation of different size classes of vertebrates is dependent on water energy and closeness to the paleo-lake shore. In addition to the preservational constraints, discovery of fossil sites is also dependent on access to relatively flat or gently sloping exposures.

Fossil mammals are generally best preserved in the middle part of the Zanda Formation at about the 170–600 m level (Fig. 4). With relatively high diversity, mammals from this segment also offer the best chronologic constraints, and the following discussions are mostly based on this assemblage. The lowest stratigraphic small mammal locality is IVPP locality ZD0609 at 174 m (from the base of the section). Of biochronologic significance are *Nannocricetus*, *Mimomys*, *Apodemus*, and *Trischizolagus mirificus*. *Nannocricetus* is present in early late Miocene through Pliocene of Inner Mongolia. Zanda Basin specimens of *Nannocricetus* are too rare to be precisely compared at the moment. Teeth of *Mimomys* are also rare. However, they are unlikely to be ancestral forms such as *Promimomys* or lophodont taxon such as *Microtodon*, the latter occurring in late Miocene. Represented by three upper first molars and one lower molar, crown heights in Zanda Basin *Mimomys* are most comparable to *Mimomys* (*Aratomys*) *bilikeensis* from early Pliocene Bilike locality of Inner Mongolia, which is the earliest representative of arvicoline rodents in China (Qiu and Storch, 2000). Arvicoline rodents first appeared in the early Pliocene of western Siberia (Repenning, 2003) and shortly afterward dispersed to northern Asia (Qiu and Storch, 2000), Europe (Fejfar et al., 1997; Chaline et al., 1999), and North America (Repenning, 1987; Lindsay et al., 2002; Bell et al., 2004). *Apodemus* has a long stratigraphic span, ranging from late Miocene to present day of Zanda Basin. Finally, *T. mirificus* is a common element at Bilike, Inner Mongolia, which is conventionally regarded as one of the earliest Pliocene faunas in north China (Qiu and Wang, 1999; Qiu et al., 2006; Z.-D. Qiu et al., in press). Zanda *T. mirificus* is indistinguishable from the Bilike form both in size and morphology, and this species is presently known in Bilike and Zanda only. Therefore, of the above four small mammals, *Mimomys* and *T. mirificus* offer the strongest chronologic constraint. Although it is possible that the Zanda *Mimomys* predates all other records of the genus in Eurasia, we think this is unlikely given a well-established record elsewhere. We thus prefer an age of earliest Pliocene to latest Miocene (but see additional discussion in Section 7, Magnetostratigraphy).

Large mammals are also mostly characterized by Pliocene elements. Carnivorans, such as *Chasmaporthetes* (IVPP localities ZD0636, 0908, 1029), *Pliohyaena* (=*Pliocrocuta*) (IVPP locality ZD1208), *Vulpes* (IVPP localities ZD1001, 1055), *Nyctereutes* (IVPP localities ZD0624, 1208), and *Meles* (IVPP localities ZD1001, 1004, 1208), are all typical Yushean taxa, even though most of these are stratigraphically 30 to more than 200 m higher than the lowest *Mimomys* horizons (IVPP locality ZD0609). The Asiatic first occurrences of these genera, some of them (such as canids) as immigrants from North America, are mostly confined in Pliocene, although occasional late Miocene records have been suggested elsewhere (Qiu, 1987; Qiu and Tedford, 1990; Tedford and Qiu, 1991; Qiu et al., 2004; Tedford et al., 2009). Other than some Miocene left overs, such as *Qurliqnoria*, ungulates collectively have a Pliocene characteristic as well.

Stratigraphically below IVPP locality ZD0609 (174 m), there are only a handful of localities producing five mammal taxa: *Ochotona*, *Panthera*, *Qurliqnoria*, *Palaeotragus*, and *Hipparion*. These are known in late Miocene of either north China (*Ochotona*, *Palaeotragus*, *Hipparion*) (Z.-X. Qiu et al., in press) or Tibetan Plateau (*Qurliqnoria*) (Wang et al., in press-b), or there are no prior record (*Panthera*). Mammals from the lower section thus offer no strong age constraint, except being consistent with a late Miocene age.

Fossil localities above the 620 m level are even fewer. Only two identifiable taxa are present: *Equus* and an advanced cervid. *Equus*, in particular, is a North American immigrant first appearing at the beginning of the Pleistocene and widely seen in northern China (Qiu, 2006) and in south Asia and Europe (Lindsay et al., 1980). Despite the paucity of fossils, the upper 180 m of Zanda Formation must thus be Pleistocene in age.

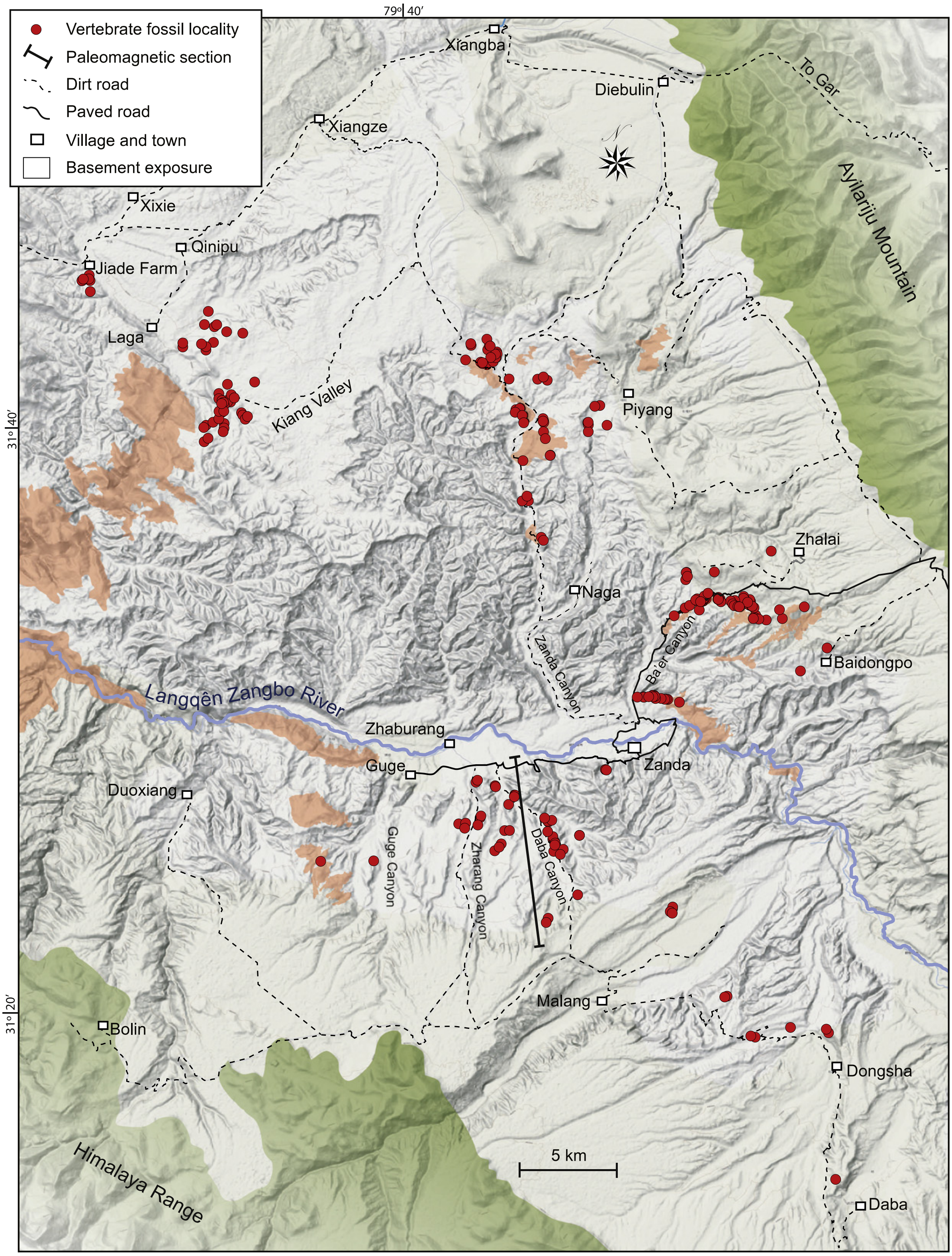

Fig. 2. Map showing important fossil localities and geographic locations discussed in the text. Vertebrate fossil sites are frequently adjacent to exposures of Tethyan basement rock (here colored in brown).

Fossil fishes occur throughout the Zanda section in fine-grained fluvial or lacustrine sediments. Studies of Tibetan fossil fishes in the Pliocene are just beginning (Chang et al., 2008; Wang and Chang, 2010, 2012). They may be of great value in paleoenvironmental, evolutionary, and zoogeographic pursuits, but so far cannot offer any insight into the geochronology.

7. Magnetostratigraphy

There have been at least three independent paleomagnetic studies of the Zanda Basin strata during the past 13 years (Qian, 1999; Saylor, 2008; Wang et al., 2008b). In addition, Zhu et al. (2005) and Meng et al. (2004) alluded to a fourth paleomagnetic section of their own, but no

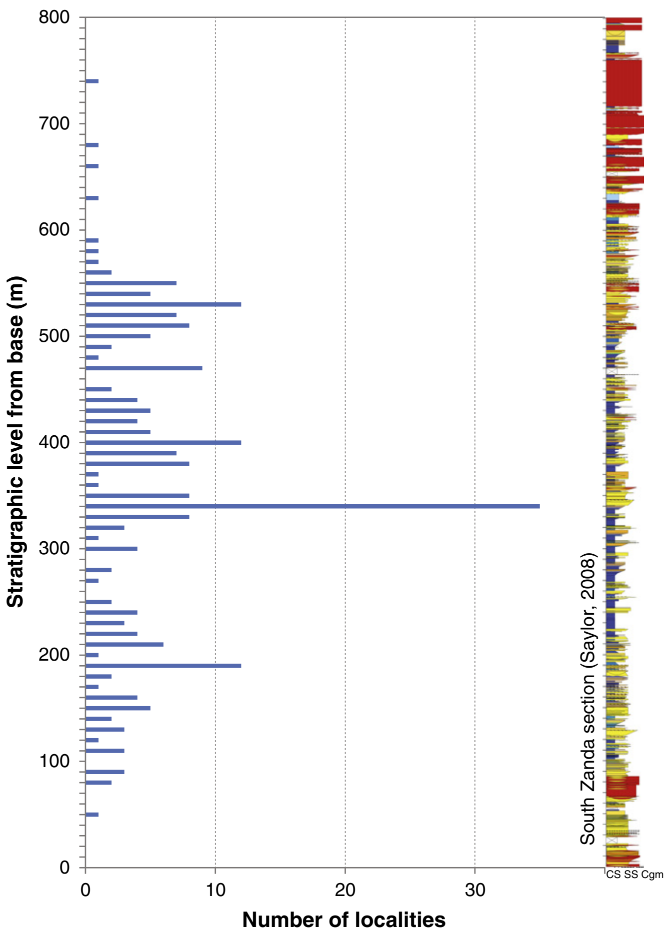

Fig. 3. Histogram showing relative abundance of vertebrate fossil localities along the 800 m section. Individual fossil localities are interpolated into six nearest measured sections, which are in turn correlated to the main south Zanda section by lithostratigraphic and sequence stratigraphic means (Saylor et al., 2010b).

documentation was provided. All three published studies obtained an 800 + m section for the total thickness of Zanda Basin sediments, and arrived at roughly similar magnetic reversal patterns.

Qian's (1999) first attempt simply correlated his magnetic section at the Xiangze area, with 12 normal and 13 reversed magnetozones, to then "Chron 6" through Jaramillo Chron (6.15–1.5 Ma). Qian's selection of the Xiangze area may have been influenced by the presence of the fossil giraffe reported by Zhang et al. (1981), although he did not explicitly use this fossil as a constraint.

Wang et al. (2008b) listed four fossil sites in their more densely sampled magnetic section revealing 15 normal and 15 reversed magnetozones that are correlated to 2An–4Ar (9.5–2.6 Ma). Of their four fossil constraints, three are mammals (*Hipparion zandaense*, *Ochotona* sp., and Dicerorhininae) and a fourth included four species of gastropods. However, of the three mammals they mentioned, only one site yielded identifiable mammals (four cheek teeth of *H. zandaense*) collected by the authors, and the other two are inferred occurrences of *Ochotona* sp. (a single cheek tooth in Meng et al., 2005) and a rhinoceros (a metapodial in Meng et al., 2004) purportedly collected from the Dingdingka area, which is across the Langqên Zangbo River many km north of Wang et al.'s (2008b) magnetic section. More importantly, the latter two fossils are not well-preserved enough to offer meaningful constraints within their proposed age range of late Miocene through Pliocene. *H. zandaense*, on the other hand, occurs only in Zanda Basin and its age is thus not externally referenced. In fact, as our own biostratigraphy shows (Figs. 4, 5), *H. zandaense* has a long range that spans from late Miocene through Pliocene. In general, the three fossil mammals (two of them lacking precise stratigraphic occurrence) cited by Wang et al. (2008b) can only serve as a weak age constraint in the range of late Miocene to Pliocene, too wide to be of much utility in a basin that straddles the entire age range. As discussed below, Wang et al.'s (2008b) correlation misplaced the Pleistocene part of the section and yielded age estimates that are about 2 Ma too old.

Most recently, Saylor et al. (2009) presented two more magnetic sections from the south and southeast Zanda Basin. A composite magnetic column was derived by combining parts of the sections with more magnetozones, and resulted in a total of 12 normal and 12 reversed zones. Saylor et al.'s south Zanda magnetic section was sampled from the same Zharang Canyon as that by Wang et al. (2008b), i.e., Zanda–Bolin section in Kempf et al. (2009), although individual measured segments (legs) differ from each other. It is thus reassuring that these two magnetic sections complement each other in many features. Where Saylor et al. (2009) under-sampled at their 100–150 m level, Wang et al.'s much denser sampling revealed a relatively long reversed zone missed by Saylor et al. (2009) (Fig. 5).

Both Qian (1999) and Saylor et al. (2009, 2010b) arrived at similar magnetic correlations in their upper sections. Saylor et al. started their top normal magnetic zone at C1n, whereas Qian, missing a normal at his top section, begins the long reversed at C1r. This is in contrast to Wang et al. (2008b) who placed his top normal (N1) in 2An. Both Wang et al. (2008b) and Saylor et al. (2009, 2010b), however, arrived at a similar correlation in the lower part of their sections (the onset of sedimentation), despite their differences in the upper sections. For chronologic constraints, Saylor et al. (2009) also used past reports of vertebrate fossils (*Hipparion*, *Palaeotragus*, etc.), as well as invoking a regional C3/C4 vegetation transition at ~7 Ma (e.g., Quade et al., 1989; France-Lanord and Derry, 1994; Quade and Cerling, 1995; Quade et al., 1995; Garzione et al., 2000; Ojha et al., 2000; Behrensmeyer et al., 2007; Ojha et al., 2009), to argue their case of a late Miocene through Pleistocene correlation of ~9.2 to < 1 Ma.

As discussed above, our own mammalian assemblages offer an independent set of age constraints. Importantly, in the lower part of the sequence, we have recovered a small mammal assemblage (IVPP localities ZD0609 and 0904) that falls in the 174–186 m level of Saylor et al.'s (Saylor, 2008; Saylor et al., 2009) south Zanda section within the top part of an alternating greenish sandstone and silt unit and just below the fine-grained lacustrine mudstones with fine laminations. Furthermore, two localities in the top section that produce *Equus* also help to anchor that part of the section to the Pleistocene.

Overall, the fossiliferous middle Zanda sequence yields characteristic Pliocene faunas with few Miocene leftovers, although the upper alluvial conglomerates and lower fluvial sandstones, from which few vertebrate fossils are found thus far, must have ranged into the Pleistocene and late Miocene, respectively. Based on our paleontologic perspective, we re-interpreted previously published paleomagnetic columns from various parts of the basin (Table 2; Fig. 5). The top 180 m (620–800 m) section with *Equus* is securely placed in the Pleistocene part (C1n–C2r) of the GPTS, as had been similarly correlated by Qian (1999) and Saylor et al. (2009). Such a correlation implies that both Wang et al. (2008b) and Saylor et al. (2009) had missed the very short normal chrons (C1r.1n, Jaramillo, and C1r.2n, Cobb Mountain) in the 667–744 m range, something not unexpected because of the extremely coarse-grained nature of that part of the section. Qian (1999), on the other hand, appears to have sampled at least one of the short chrons (Fig. 5). Our correlations in the next two major magnetochrons (C2An and C2Ar) below the Pleistocene section also agree with that by Saylor et al. (2009), making the upper half (400 m and up) of the Zanda section relatively uncontroversial in chronology, although a brief reversed zone (R3) in Wang et al. (2008b) must be left unexplained.

The lower half of the composite, however, is less satisfactorily resolved. Significantly, the most severe constraint is placed on the normal interval that contains IVPP locality ZD0609, which produced a small mammal fauna that is Pliocene in character, and we have elevated it to

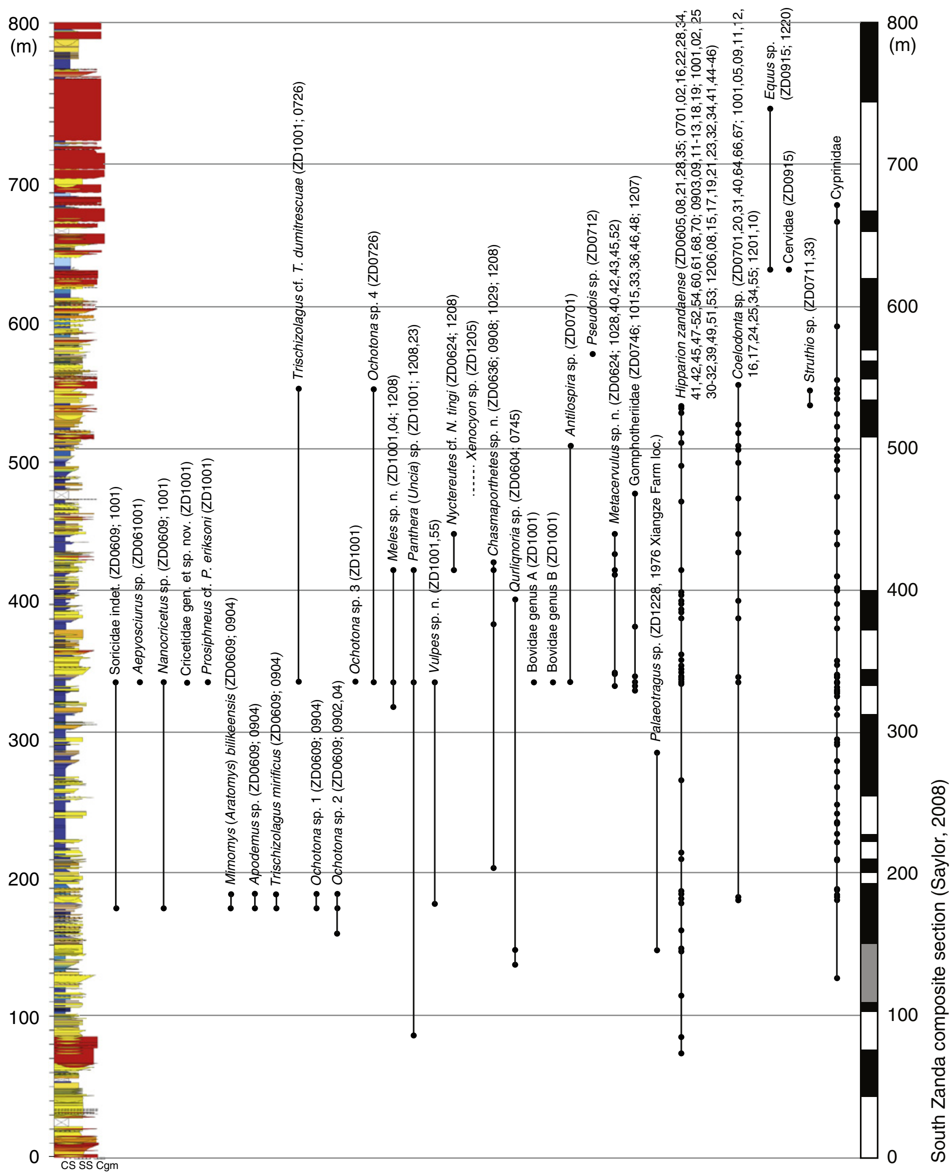

Fig. 4. Biostratigraphy of Zanda vertebrates, based on data from Tables 1 and 3. Individual fossil localities (solid circles) are interpolated into six nearest measured sections, which are in turn correlated to the main south Zanda section by lithostratigraphic and sequence stratigraphic means (Saylor et al., 2010b). For additional explanations, see caption of Table 3.

C3n.4n. Such a correlation has a cascading effect of moving the next few magnetozones upward, compressing the lower 200–400 m section into a relatively short interval around C3n. Our new age estimates of the Zanda section (Fig. 5) thus span ~400 Ka to 6.4 Ma using the GPTS of ATNTS2004 (Lourens et al., 2004). Our correlation has the undesirable effect of leaving unexplained several short reversals [333–345 m (N8), ~225 m (R11), and 110–120 m (N14)] observed by Saylor et al. (2009) and Wang et al. (2008b).

If we allow a more relaxed interpretation of the small mammal fauna from IVPP locality ZD0609, an alternative correlation is possible for the lower section (dashed lines in Fig. 5). This alternative correlation, more consistent with an even depositional rate, would imply that taxa such as *Mimomys* and *Trischizolagus* must have occurred ~1 Ma earlier in Zanda Basin than their known records elsewhere. Furthermore, the alternative also carries its own unexplained short magnetozones (N11 and N12 in Wang et al., 2008b). Such an alternative magnetic interpretation of C1n–C4r for Zanda strata (~400 Ka to 8.3 Ma) is closest, but not identical, to that proposed by Qian (1999) although the latter lacks adequate documentation and does not permit placement of our fossils in his section. If the alternative correlation is correct, a number of short magnetochrons (C3B) that are not seen in all three known magnetic sections may have been missed in the coarse sediments at the base of the section.

8. Zanda faunal characteristics and zoogeography

The Zanda Pliocene mammal fauna has two major components. First, many of the large and small mammals have clearly a north China affinity. Typical large mammals from north China or eastern Asian arid or semi-arid regions include *Chasmaporthetes*, *Pliohyaena* (=*Pliocrocuta*), *Meles*, *Nyctereutes*, *Xenocyon*, *Antilospira*, and *Hipparion*. Small mammals that can find their counterparts in north China include *Nannocricetus*, *Prosiphneus*, *Apodemus*, *Mimomys*, and *Trischizolagus*; these are especially abundant in the Pliocene of Inner Mongolia, located at much higher latitudes than Zanda. This is perhaps not surprising given that high

Table 1
List of vertebrate fossil localities, elevation, stratigraphic level as interpolated to nearest measured sections (Saylor et al., 2010a, 2010b), stratigraphic level relative to south Zanda measured section (m from bottom), and calibrated paleomagnetic ages (Ma). See Sections 2, 6, and 7 (Material and methods, Biostratigraphy, and Magnetostratigraphy) for explanations of correlation scheme. Ages for magnetic chrons in the Geomagnetic Polarity Time Scale (GPTS) are based on ATNTS2004 in Lourens et al. (2004).

Locality number	Canyon or washes	Elev (m)	Nearest Saylor sections	South Zanda sect (m)	GPTS	Age (Ma)
ZD0604	Zanda Basin	3803	S Zanda leg 3	131	C3r	5.46
ZD0605	Zanda Basin	3815	S Zanda leg 3	143	C3r	5.34
ZD0606	Zanda Basin	3797	S Zanda leg 3	126	C3r	5.52
ZD0607	Zanda Basin	3856	S Zanda leg 4	182	C3n.4n	5.07
ZD0608	Zanda Basin	3862	S Zanda leg 4	188	C3n.4n	5.03
ZD0609	Zanda Basin	3847	S Zanda leg 4	174	C3n.4n	5.12
ZD0610	Zanda Basin	3838	S Zanda leg 4	165	C3n.4n	5.16
ZD0611	Zanda Basin	3906	S Zanda leg 5	237	C3n.2r	4.75
ZD0612	Zanda Basin	3904	S Zanda leg 5	234	C3n.2r	4.76
ZD0613	Zanda Basin	3892	S Zanda leg 5	221	C3n.3n	4.83
ZD0614	Zanda Basin	3882	S Zanda leg 5	209	C3n.3n	4.87
ZD0615	Zanda Basin	3905	S Zanda leg 5	235	C3n.2r	4.75
ZD0616	Zanda Basin	4034	S Zanda leg 8	362	C3n.1r	4.33
ZD0617	Zanda Basin	3806	S Zanda leg 3	134	C3r	5.43
ZD0618	Zanda Basin	4205	SE Zanda leg 8	587	C2An.1n	2.87
ZD0619	Zanda Basin	4318	SE Zanda leg 9	672	C1r	1.71
ZD0620	Zanda Basin	4062	Namru Road W leg 1	313	C3n.1r	4.49
ZD0621	Zanda Basin	4104	Namru Road W leg 1	344	C3n.1r	4.39
ZD0622	Zanda Basin	4108	Namru Road W leg 1	347	C3n.1r	4.38
ZD0623	Zanda Basin	4196	Namru Road W leg 1	440	C2Ar	3.97
ZD0624	Zanda Basin	4194	Namru Road W leg 1	439	C2Ar	3.97
ZD0625	Zanda Basin	3790	S Zanda leg 3	119	C3r	5.58
ZD0626	Zanda Basin	3770	S Zanda leg 3	100	C3r	5.78
ZD0627	Zanda Basin	3857	S Zanda leg 4	183	C3n.4n	5.06
ZD0628	Zanda Basin	3857	S Zanda leg 4	183	C3n.4n	5.06
ZD0629	Zanda Basin	3898	S Zanda leg 5	227	C3n.3n	4.80
ZD0630	Zanda Basin	3864	S Zanda leg 4	190	C3n.4n	5.02
ZD0631	Zanda Basin	3973	S Zanda leg 7	302	C3n.2n	4.52
ZD0632	Zanda Basin	3916	S Zanda leg 5	248	C3n.2r	4.67
ZD0633	Zanda Basin	4189	Namru Road W leg 1	433	C2Ar	4.01
ZD0634	Zanda Basin	4164	Namru Road W leg 1	398	C3n.1n	4.20
ZD0635	Zanda Basin	4168	Namru Road E leg 4	385	C3n.1n	4.25
ZD0636	Zanda Basin	4205	Namru Road E leg 4+	420	C2Ar	4.08
ZD0637	Zanda Basin	4211	Namru Road E leg 4+	424	C2Ar	4.06
ZDJS01	Zanda Basin	3830	S Zanda leg 4	157	C3n.4n	5.21
ZDJS02	Zanda Basin	3830	S Zanda leg 4	157	C3n.4n	5.21
ZDJS03	Zanda Basin	4000	E Zanda leg 3	213	C3n.3n	4.85
ZDJS04	Zanda Basin	3858	S Zanda leg 4	184	C3n.4n	5.06
ZDJS05	Zanda Basin	3743	E Zanda leg 1	50	C3An.1n	6.21
ZDJS06	Zanda Basin	3792	S Zanda leg 3	121	C3r	5.56
ZDJS07	Zanda Basin	4073	S Zanda leg 9	401	C2Ar	4.18
ZDJS08	Zanda Basin	4082	E Zanda leg 3	295	C3n.2n	4.54
ZDJS09	Zanda Basin	4131	SE Zanda leg 7	550	C2An.2n	3.19
ZD0701	Zanda Gou	4217	Namru Road E leg 4+	503	C2Ar	3.62
ZD0702	Zanda Gou	4198	Namru Road E leg 4+	487	C2Ar	3.71
ZD0703	Zanda Gou	4180	Namru Road E leg 4	472	C2Ar	3.79
ZD0704	Zanda Gou	4204	Namru Road E leg 4+	492	C2Ar	3.68
ZD0705	Zanda Gou	4157	Namru Road E leg 4	388	C3n.1n	4.24
ZD0706	Zanda Gou	4232	Namru Road E leg 4+	515	C2An.3n	3.52
ZD0707	Zanda Gou	4250	Namru Road E leg 4+	530	C2An.3n	3.36
ZD0708	Zanda Gou	4156	Namru Road E leg 4	387	C3n.1n	4.24
ZD0709	Zanda Gou	4183	Namru Road E leg 4	409	C2Ar	4.14
ZD0710	Zanda Gou	4210	Namru Road E leg 4+	497	C2Ar	3.66
ZD0711	Guanjingtai	4238	E Zanda leg 5	538	C2An.2r	3.29
ZD0712	Guanjingtai	4295	E Zanda leg 5+	568	C2An.1r	3.10
ZD0713	Guanjingtai	4208	E Zanda leg 5	506	C2Ar	3.61
ZD0714	Guanjingtai	4208	E Zanda leg 5	506	C2Ar	3.61
ZD0715	Guanjingtai	4217	E Zanda leg 5	517	C2An.3n	3.50
ZD0716	Guanjingtai	4228	E Zanda leg 5	525	C2An.3n	3.42
ZD0717	Guanjingtai	4284	E Zanda leg 5+	560	C2An.2n	3.13
ZD0718	Guanjingtai	4243	E Zanda leg 5	542	C2An.2r	3.26
ZD0719	Guanjingtai	4234	E Zanda leg 5	532	C2An.3n	3.34
ZD0720	Guanjingtai	4215	E Zanda leg 5	516	C2An.3n	3.51
ZD0721	Guanjingtai	4251	E Zanda leg 5	547	C2An.2r	3.22
ZD0722	Guanjingtai	4228	E Zanda leg 5	525	C2An.3n	3.42
ZD0723	Guanjingtai	4221	E Zanda leg 5	523	C2An.3n	3.44
ZD0724	Guanjingtai	4222	E Zanda leg 5	524	C2An.3n	3.43
ZD0725	Guanjingtai	4247	E Zanda leg 5	543	C2An.2r	3.25
ZD0726	Guanjingtai	4245	E Zanda leg 5	542	C2An.2r	3.26
ZD0727	Guanjingtai	3920	E Zanda leg 3	188	C3n.4n	5.04
ZD0728	Guanjingtai	3910	E Zanda leg 3	185	C3n.4n	5.05
ZD0729	Guanjingtai	3909	E Zanda leg 3	184	C3n.4n	5.06

Table 1 (*continued*)

Locality number	Canyon or washes	Elev (m)	Nearest Saylor sections	South Zanda sect (m)	GPTS	Age (Ma)
ZD0730	Guanjingtai	4231	E Zanda leg 5	530	C2An.3n	3.36
ZD0731	Guanjingtai	4262	E Zanda leg 5+	545	C2An.2r	3.23
ZD0732	Guanjingtai	4243	E Zanda leg 5	542	C2An.2r	3.26
ZD0733	Guanjingtai	4229	E Zanda leg 5	528	C2An.3n	3.38
ZD0734	Guanjingtai	4229	E Zanda leg 5	528	C2An.3n	3.38
ZD0735	Guanjingtai	4237	E Zanda leg 5	537	C2An.2r	3.30
ZD0736	Guanjingtai	4229	E Zanda leg 5	528	C2An.3n	3.38
ZD0737	Guanjingtai	4190	E Zanda leg 4	427	C2Ar	4.04
ZD0738	Guanjingtai	4192	E Zanda leg 4	429	C2Ar	4.03
ZD0739	Guge Gou	4017	Guge leg 5	328	C3n.1r	4.44
ZD0740	Guanjingtai	4207	E Zanda leg 5	490	C2Ar	3.69
ZD0741	Guanjingtai	4198	E Zanda leg 4	464	C2Ar	3.84
ZD0742	Guanjingtai	4196	E Zanda leg 4	462	C2Ar	3.85
ZD0743	Zhalai	4394	E Zanda leg 5+	660	C2n	1.86
ZD0744	Daba Gou	3903	E Zanda leg 3	185	C3n.4n	5.05
ZD0745	Guanjingtai	4161	E Zanda leg 4	393	C3n.1n	4.22
ZD0746	Guanjingtai	4129	E Zanda leg 3–4	337	C3n.1r	4.41
ZD0747	Guanjingtai	4159	E Zanda leg 4	391	C3n.1n	4.22
ZD0748	Guanjingtai	4123	E Zanda leg 3–4	338	C3n.1r	4.41
ZD0749	Guanjingtai	4145	E Zanda leg 4	380	C3n.1n	4.27
ZD0750	Guanjingtai	4150	E Zanda leg 4	385	C3n.1n	4.25
ZD0751	Guanjingtai	4169	E Zanda leg 4	399	C3n.1n	4.19
ZD0752	Guanjingtai	4165	E Zanda leg 4	396	C3n.1n	4.20
ZD0753	Guanjingtai	4102	E Zanda leg 3	317	C3n.1r	4.48
ZD0754	Guanjingtai	4162	E Zanda leg 4	393	C3n.1n	4.22
ZD0755	Guanjingtai	4113	E Zanda leg 3	329	C3n.1r	4.44
ZD0756	Guanjingtai	4109	E Zanda leg 3	325	C3n.1r	4.45
ZD0757	Guanjingtai	4125	E Zanda leg 3–4	340	C3n.1r	4.40
ZD0758	Guanjingtai	4138	E Zanda leg 4	374	C3n.1n	4.29
ZD0759	Guanjingtai	4131	E Zanda leg 4	340	C3n.1r	4.40
ZD0760	Guanjingtai	4155	E Zanda leg 4	390	C3n.1n	4.23
ZD0761	Guanjingtai	4158	E Zanda leg 4	393	C3n.1n	4.22
ZD0762	Guanjingtai	4168	E Zanda leg 4	400	C2Ar	4.19
ZD0763	Guanjingtai	4171	E Zanda leg 4	402	C2Ar	4.18
ZD0764	Guanjingtai	4193	E Zanda leg 4	440	C2Ar	3.97
ZD0765	Guanjingtai	4197	E Zanda leg 4	444	C2Ar	3.95
ZD0766	Guanjingtai	4121	E Zanda leg 3–4	335	C3n.1r	4.42
ZD0767	Guanjingtai	4141	E Zanda leg 4	379	C3n.1n	4.27
ZD0768	Xiangzi SW	4100	Namru Road E leg 3–4	338	C3n.1r	4.41
ZD0769	Xiangzi SW	4141	Namru Road E leg 4	374	C3n.1n	4.29
ZD0770	Xiangzi SW	4108	Namru Road E leg 3–4	335	C3n.1r	4.42
ZD0771	Xiangzi SW	4124	Namru Road E leg 3–4	340	C3n.1r	4.40
ZD0901	Daba Gou	3791	S Zanda leg 3	120	C3r	5.57
ZD0902	Daba Gou	3832	S Zanda leg 4	159	C3n.4n	5.20
ZD0903	Daba Gou	3854	S Zanda leg 4	180	C3n.4n	5.08
ZD0904	Daba Gou	3860	S Zanda leg 4	186	C3n.4n	5.05
ZD0905	Daba Gou	3964	S Zanda leg 6	293	C3n.2n	4.54
ZD0906	Daba Gou	3905	S Zanda leg 5	236	C3n.2r	4.75
ZD0907	Daba Gou	3882	S Zanda leg 5	210	C3n.3n	4.87
ZD0908	Zanda Gou	3853	Namru Road E leg 3	203	C3n.3n	4.89
ZD0909	Daba Gou	3882	S Zanda leg 5	210	C3n.3n	4.87
ZD0910	Zanda Gou	3873	Namru Road E leg 3	205	C3n.3n	4.88
ZD0911	Zanda Gou	3927	Namru Road E leg 3	214	C3n.3n	4.85
ZD0912	Zanda Gou	3901	Namru Road E leg 3	213	C3n.3n	4.85
ZD0913	Zanda Gou	3903	Namru Road E leg 3	213	C3n.3n	4.85
ZD0914	Zanda Gou	3948	Namru Road E leg 3	230	C3n.2r	4.79
ZD0915	Nama	4244	SE Zanda leg 9	625	C2r	2.48
ZD0916	Nama	4173	S Zanda leg 9	501	C2Ar	3.63
ZD0917	Daba Gou	4186	S Zanda leg 9	514	C2An.3n	3.53
ZD0918	Daba Gou	3937	S Zanda leg 6	267	C3n.2n	4.60
ZD0919	Daba Gou	4027	S Zanda leg 8	355	C3n.1r	4.36
ZD0920	Daba Gou	3942	S Zanda leg 6	272	C3n.2n	4.59
ZD1001	Zanda Gou	4114	Namru Road E leg 3–4	335	C3n.1r	4.42
ZD1002	Zanda Gou	4113	Namru Road E leg 3–4	335	C3n.1r	4.42
ZD1003	Zanda Gou	4121	Namru Road E leg 3–4	338	C3n.1r	4.41
ZD1004	Zanda Gou	4064	Namru Road E leg 3–4	318	C3n.1r	4.48
ZD1005	Zanda Gou	4105	Namru Road E leg 3–4	335	C3n.1r	4.42
ZD1006	Zanda Gou	4183	Namru Road E leg 4	419	C2Ar	4.08
ZD1007	Zanda Gou	4144	Namru Road E leg 4	340	C3n.1r	4.40
ZD1008	Zanda Gou	4165	Namru Road E leg 4	391	C3n.1n	4.22
ZD1009	Zanda Gou	4118	Namru Road E leg 3–4	338	C3n.1r	4.41
ZD1010	Zanda Gou	4105	Namru Road E leg 3–4	335	C3n.1r	4.42
ZD1011	Zanda Gou	4195	Namru Road E leg 4+	425	C2Ar	4.05
ZD1012	Zanda Gou	4163	Namru Road E leg 4	393	C3n.1n	4.22
ZD1013	Zanda Gou	4206	Namru Road E leg 4+	450	C2Ar	3.91

(*continued on next page*)

Table 1 (*continued*)

Locality number	Canyon or washes	Elev (m)	Nearest Saylor sections	South Zanda sect (m)	GPTS	Age (Ma)
ZD1014	Zanda Gou	3881	Namru Road E leg 3	205	C3n.3n	4.88
ZD1015	Zanda Gou	4122	Namru Road E leg 3–4	339	C3n.1r	4.41
ZD1016	Zanda Gou	4120	Namru Road E leg 3–4	339	C3n.1r	4.41
ZD1017	Piyang	4156	Namru Road E leg 4	389	C3n.1n	4.23
ZD1018	Piyang	4213	Namru Road E leg 4+	467	C2Ar	3.82
ZD1019	Piyang	4210	Namru Road E leg 4+	467	C2Ar	3.82
ZD1020	Piyang	4232	Namru Road E leg 4+	516	C2An.3n	3.51
ZD1021	Piyang	4206	Namru Road E leg 4+	466	C2Ar	3.83
ZD1022	Piyang	4169	Namru Road E leg 4	395	C3n.1n	4.21
ZD1023	Piyang	4153	Namru Road E leg 4	385	C3n.1n	4.25
ZD1024	Zanda Gou	4097	Namru Road E leg 3–4	335	C3n.1r	4.42
ZD1025	Ba'er Gou	3893	E Zanda leg 2	183	C3n.4n	5.06
ZD1026	Kiang Valley	4098	Namru Road E leg 3–4	335	C3n.1r	4.42
ZD1027	Kiang Valley	4133	Namru Road E leg 4	373	C3n.1n	4.30
ZD1028	Kiang Valley	4129	Namru Road E leg 4	340	C3n.1r	4.40
ZD1029	Kiang Valley	4138	Namru Road E leg 4	375	C3n.1n	4.29
ZD1030	Kiang Valley	4102	Namru Road E leg 3–4	336	C3n.1r	4.42
ZD1031	Kiang Valley	4102	Namru Road E leg 3–4	336	C3n.1r	4.42
ZD1032	Kiang Valley	4096	Namru Road E leg 3–4	335	C3n.1r	4.42
ZD1033	Kiang Valley	4109	Namru Road E leg 3–4	375	C3n.1n	4.29
ZD1034	Kiang Valley	4100	Namru Road E leg 3–4	336	C3n.1r	4.42
ZD1035	Kiang Valley	4088	Namru Road E leg 3–4	334	C3n.1r	4.42
ZD1036	Kiang Valley	4067	Namru Road E leg 3–4	329	C3n.1r	4.44
ZD1037	Kiang Valley	4071	Namru Road E leg 3–4	330	C3n.1r	4.44
ZD1038	Kiang Valley	4085	Namru Road E leg 3–4	331	C3n.1r	4.43
ZD1039	Kiang Valley	4223	Namru Road E leg 4+	510	C2An.3n	3.57
ZD1040	Kiang Valley	4186	Namru Road E leg 4	410	C2Ar	4.13
ZD1041	Kiang Valley	4065	Namru Road E leg 3–4	327	C3n.1r	4.45
ZD1042	Kiang Valley	4188	Namru Road E leg 4	411	C2Ar	4.13
ZD1043	Kiang Valley	4196	Namru Road E leg 4+	425	C2Ar	4.05
ZD1044	Kiang Valley	4162	Namru Road E leg 4	393	C3n.1n	4.22
ZD1045	Kiang Valley	4130	Namru Road E leg 4	341	C3n.1r	4.40
ZD1046	Kiang Valley	4083	Namru Road E leg 3–4	332	C3n.1r	4.43
ZD1047	Kiang Valley	4096	Namru Road E leg 3–4	336	C3n.1r	4.42
ZD1048	Kiang Valley	4089	Namru Road E leg 3–4	334	C3n.1r	4.42
ZD1049	Kiang Valley	4077	Namru Road E leg 3–4	330	C3n.1r	4.44
ZD1050	Kiang Valley	4104	Namru Road E leg 3–4	336	C3n.1r	4.42
ZD1051	Kiang Valley	4108	Namru Road E leg 3–4	338	C3n.1r	4.41
ZD1052	Kiang Valley	4084	Namru Road E leg 3–4	332	C3n.1r	4.43
ZD1053	Ba'er Gou	3856	E Zanda leg 2	147	C3r	5.29
ZD1055	Ba'er Gou	3880	E Zanda leg 2	180	C3n.4n	5.08
ZD1056	Kiang Valley	4084	Namru Road E leg 3–4	332	C3n.1r	4.43
ZD1201	Ba'er Gou	3846	E Zanda leg 2	132	C3r	5.45
ZD1202	Ba'er Gou	3857	E Zanda leg 2	147	C3r	5.29
ZD1203	Guge Gou	4205	Guge leg 7	575	C2An.1n	2.98
ZD1204	Daba Gou	4118	SE Zanda leg 6	535	C2An.2r	3.31
ZD1205	Daba Gou	4045	SE Zanda leg 6	469	C2Ar	3.81
ZD1206	Daba Gou	4043	SE Zanda leg 6	467	C2Ar	3.82
ZD1207	Daba Gou	4044	SE Zanda leg 6	468	C2Ar	3.81
ZD1208	Zanda Gou	4195	Namru Road E leg 4+	415	C2Ar	4.10
ZD1209	Zanda Gou	4125	Namru Road E leg 4	340	C3n.1r	4.40
ZD1210	Zanda Gou	4240	Namru Road E leg 4+	510	C2An.3n	3.57
ZD1211	Zanda Gou	4239	Namru Road E leg 4+	509	C2An.3n	3.59
ZD1212	Zanda Gou	4251	Namru Road E leg 4+	515	C2An.3n	3.52
ZD1213	Zanda Gou	4188	Namru Road E leg 4	410	C2Ar	4.13
ZD1214	Ba'er Gou	4203	E Zanda leg 4	495	C2Ar	3.67
ZD1215	Ba'er Gou	4196	E Zanda leg 4	467	C2Ar	3.82
ZD1216	Ba'er Gou	4270	E Zanda leg 5+	560	C2An.2n	3.13
ZD1217	Ba'er Gou	4208	E Zanda leg 5	500	C2Ar	3.64
ZD1218	Ba'er Gou	4217	E Zanda leg 5	517	C2An.3n	3.50
ZD1219	Ba'er Gou	4209	E Zanda leg 5	501	C2Ar	3.63
ZD1220	Ba'er Gou	4399	E Zanda leg 5+	740	C1r	0.83
ZD1221	Ba'er Gou	3840	E Zanda leg 2	110	C3r	5.68
ZD1222	Ba'er Gou	3849	E Zanda leg 2	145	C3r	5.31
ZD1223	Ba'er Gou	3823	E Zanda leg 2	85	C3r	5.95
ZD1224	Ba'er Gou	3816	E Zanda leg 2	75	C3An.1n	6.05
ZD1225	Ba'er Gou	3813	E Zanda leg 2	73	C3An.1n	6.06
ZD1226	Ba'er Gou	3821	E Zanda leg 2	83	C3r	5.97
ZD1227	Ba'er Gou	3866	E Zanda leg 2	160	C3n.4n	5.19
ZD1228	Ba'er Gou	3850	E Zanda leg 2	146	C3r	5.30
ZD1229	Ba'er Gou	3826	E Zanda leg 2	87	C3r	5.93
ZD1230	Ba'er Gou	3840	E Zanda leg 2	110	C3r	5.68
ZD1231	Baicun	4227	E Zanda leg 5	528	C2An.3n	3.38
ZD1232	Mangnang N	4107	SE Zanda leg 6	530	C2An.3n	3.36
ZD1233	Mangnang N	4116	SE Zanda leg 6	535	C2An.2r	3.31
ZD1234	Mangnang N	4096	SE Zanda leg 6	525	C2An.3n	3.42

Table 1 (*continued*)

Locality number	Canyon or washes	Elev (m)	Nearest Saylor sections	South Zanda sect (m)	GPTS	Age (Ma)
ZD1235	Baicun	4046	E Zanda leg 3	243	C3n.2r	4.71
ZD1236	Laga Village	4135	Namru Road E leg 4	380	C3n.1n	4.27
ZD1237	Laga Village	3992	Namru Road E leg 3–4	280	C3n.2n	4.57
ZD1238	Laga Village	4215	Namru Road E leg 4+	500	C2Ar	3.64
ZD1239	Laga Village	4071	Namru Road E leg 3–4	330	C3n.1r	4.44
ZD1240	Laga Village	4078	Namru Road E leg 3–4	334	C3n.1r	4.42
ZD1241	Laga Village	4108	Namru Road E leg 3–4	350	C3n.1r	4.37
ZD1242	Laga Village	4022	Namru Road E leg 3–4	295	C3n.2n	4.54
ZD1243	Laga Village	4107	Namru Road E leg 3–4	350	C3n.1r	4.37
ZD1244	Laga Village	4110	Namru Road E leg 3–4	350	C3n.1r	4.37
ZD1245	Laga Village	4099	Namru Road E leg 3–4	345	C3n.1r	4.39
ZD1246	Laga Village	4094	Namru Road E leg 3–4	342	C3n.1r	4.40
ZD1247	Laga Village	4016	Namru Road E leg 3–4	292	C3n.2n	4.54

altitudes in Tibet translate to a climate much colder than its equivalent latitudes elsewhere.

The second group consists of native Tibetan components in the fauna. These include *Qurliqnoria*, *Pseudois*, and possibly *Panthera* for large mammals and *Aepyosciurus* and several species of *Ochotona* for small mammals. *Qurliqnoria*, mostly confined to the Tibetan Plateau, first appeared in the late Miocene of Qaidam Basin (Bohlin, 1937; Wang et al., 2007; X. Wang et al., 2011) and may have given rise

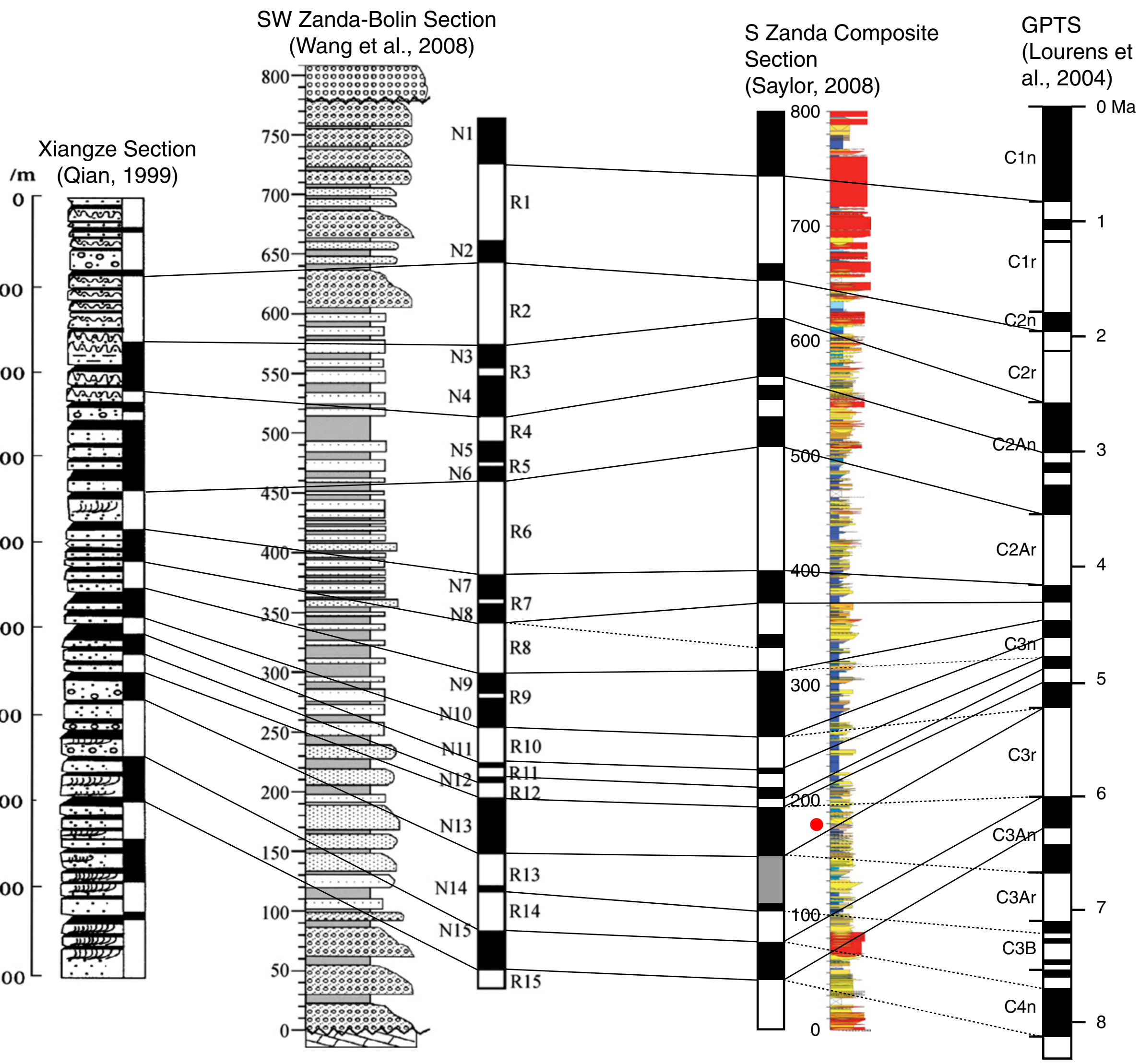

Fig. 5. Correlation of three published paleomagnetic sections. Red circle indicate key fossil sites (ZD0609, 0904) for biochronologic constraints. Ages for magnetic chrons in the Geomagnetic Polarity Time Scale (GPTS) are based on ATNTS2004 in Lourens et al. (2004).

Table 2
Alternative correlations of south Zanda magnetic sections with magnetic chrons in the Geomagnetic Polarity Time Scale (GPTS) based on ATNTS2004 in Lourens et al. (2004).

South Zhada section of Saylor 2010	Correlation with magnetozones in Wang et al. 2008	Preferred correlation based on constraints of large and small mammals		An alternative correlation with lower section proportional to strata thickness	
Meters above base of section		GPTS 2004	Range in Ma	GPTS 2004	Range in Ma
800–744	N1	C1n	0–0.781	C1n	0–0.781
744–667	R1	C1r	0.781–1.778	C1r	0.781–1.778
667–652	N2	C2n	1.778–1.945	C2n	1.778–1.945
652–620	R2	C2r	1.945–2.581	C2r	1.945–2.581
620–569	N3–N4	C2An.1n	2.581–3.032	C2An.1n	2.581–3.032
569–562	R4	C2An.1r	3.032–3.116	C2An.1r	3.032–3.116
562–548	N5	C2An.2n	3.116–3.207	C2An.2n	3.116–3.207
548–533	R5	C2An.2r	3.207–3.330	C2An.2r	3.207–3.330
533–508	N6	C2An.3n	3.330–3.596	C2An.3n	3.330–3.596
508–400	R6	C2Ar	3.596–4.187	C2Ar	3.596–4.187
400–372	N7–N8	C3n.1n	4.187–4.300	C3n.1n	4.187–4.300
372–345	R8	C3n.1r	4.300–4.493	C3n.1r	4.300–4.493
345–333	R8	C3n.1r	4.300–4.493	C3n.2n	4.493–4.631
333–313	R8	C3n.1r	4.300–4.493	C3n.2r	4.631–4.799
313–255	N9–N10	C3n.2n	4.493–4.631	C3n.3n–C3n.4n	4.799–5.235
255–228	R10	C3n.2r	4.631–4.799	C3r	5.235–6.033
228–223	N11	C3n.3n	4.799–4.896	C3r	5.235–6.033
223–211	R11	C3n.3n	4.799–4.896	C3r	5.235–6.033
211–202	N12	C3n.3n	4.799–4.896	C3r	5.235–6.033
202–195	R12	C3n.3r	4.896–4.997	C3r	5.235–6.033
195–152	N13	C3n.4n	4.997–5.235	C3An	6.033–6.733
152–110	R13	C3r	5.235–6.033	C3Ar	6.733–7.140
110–104	N14	C3r	5.235–6.033	C3Bn	7.140–7.212
104–77	R14	C3r	5.235–6.033	C3Br–C4n.1r	7.212–7.695
77–44	N15	C3An.1n	6.033–6.252	C4n.2n	7.695–8.108
44–0	R15	C3An.1r	6.252–6.436	C4r.1r	8.108–8.254

to the modern Tibetan antelope (Chiru) *Pantholops hodgsonii* (Gentry, 1968). The Blue Sheep, *Pseudois*, is another native Tibetan basal caprine possibly related to pantholopines (Fernández and Vrba, 2005).

We chose to not subdivide the Zanda Pliocene fauna for the moment. There is an apparent small mammal faunal turnover from IVPP localities ZD0609/0904 (5.12–5.05 Ma) to ZD1001 (4.42 Ma), recording a change from *Trischizolagus mirificus* to *T. dumitrescuae* and various species of *Ochotona*, but because of the scarcity of small mammal localities, it is not clear how much of this is due to a sampling effect.

Additional collecting in Zanda Basin will surely extend the ranges of many taxa, and our local first appearance and last appearance datum (Table 3) should only be considered as tentative. For example, we consider it likely that *Qurliqnoria* should extend down through the late Miocene because it has been known in early late Miocene in Qaidam Basin (Wang et al., 2007; X. Wang et al., 2011). Similarly, *Palaeotragus* likely had a deeper history because it has been reported in Gyirong Basin (Huang et al., 1980; Wang et al., in press-b), whose *Hipparion* fauna has been dated to 7.0–6.7 Ma (Yue et al., 2004).

In the Pleistocene part of the section (the upper 180 m), an *Equus* fauna is emerging even though the very coarse-grained sediments reveal no more than a handful of localities producing very fragmentary materials. Of these, we can recognize some *Equus* limb bones and a deer antler fragment that appears to be more advanced than those seen in the Pliocene part of the section. Nonetheless, the local first appearance of *Equus* (IVPP locality ZD0915, 625 m, 2.48 Ma) is close to the beginning of the Pleistocene, indicating a rapid spread of the monodactylid horse as soon as it arrived in the Old World (Lindsay et al., 1980), highlighting its usefulness as a biochron. Therefore, despite the scarcity of fossil sites in the upper Zanda section, there is definitively observable faunal turnover at the Plio-Pleistocene boundary around the 620 m level.

The three-toed horse *Hipparion zandaense*, on the other hand, is the most densely sampled of any mammal species in Zanda (55 localities; Table 3). Between its last appearance datum (IVPP locality ZD1232, 530 m, 3.36 Ma) and the first appearance of *Equus*, however, there is a long hiatus with poor sampling. This 0.8 myr gap is clearly a result of unfossiliferous coarse-grained sediments, and consequently we are unable to address the issue of how closely *Equus* locally replaced *Hipparion*.

If a more relaxed interpretation of the biochronology of Zanda small mammals is taken, allowing taxa such as *Mimomys* and *Trischizolagus* to extend their ranges into the late Miocene (dashed lines in Fig. 5), then our "out of Tibet" hypothesis can also be applied to the small mammals. However, such a tantalizing prospect will have to await the full study of the small mammal fauna.

9. Conclusion

The late Miocene to Pleistocene Zanda Basin is uniquely situated at the northern foothills of the Himalayas and preserves an excellent record of fossil mammals and fishes. This is the best record so far known in Tibet, especially in its exceptionally preserved Pliocene mammal assemblages. The 800 m sedimentary sequence is essentially continuous, often fine-grained, and is ideal for archiving both fishes and terrestrial mammals.

Despite the current preliminary stage of exploration, the Zanda fossil assemblage has revealed an ancestral wooly rhino that was the precursor of its late Pleistocene megafaunal descendants. Such a discovery highlights our "out of Tibet" hypothesis of Pliocene high Tibet as a "training ground" for cold adaptations.

A detailed biostratigraphy based on fossil mammals is presented. Individual localities are correlated to an 800 m master lithostratigraphic and magnetic section, offering a unified, basin-wide framework of superposition. Correlations of individual fossil sites have an error range of about $\pm$ 20 m or less, or $\pm$ 0.2 myr in age range. This high-resolution biostratigraphy thus provides, for the first time, a window into the past biological world.

The new Zanda mammal assemblage provides a far stronger biochronologic constraint than has so far been possible. Using its

Table 3
Local first and last appearances (FAD and LAD) of Zanda vertebrates and individual Zanda (ZD) localities. In cases where there are more than two localities, locality numbers for the first and last appearances are indicated by bold type. See Fig. 4 and Table 1 for complete listing of all localities. For two of the more densely sampled taxa, *Hipparion zandaense* and *Coelodonta thibetana*, many of the localities produced postcranial or poorly preserved cranial and dental materials and identifications to species level is often not possible. Since only one three-toed horse and one rhinoceros are so far known, we tentatively include all localities with less identifiable materials within these two species, which are treated in the same way in Fig. 4. Ages for magnetic chrons in the Geomagnetic Polarity Time Scale (GPTS) are based on ATNTS2004 in Lourens et al. (2004).

Taxa	FAD (Ma)	LAD (Ma)	Localities
Rodentia			
Soricidae indet.	5.12	4.42	ZD0609, 1001
Aepyosciurus sp.	4.42	4.42	ZD1001
Nannocricetus sp.	5.12	4.42	ZD0609, 1001
Cricetidae gen. et sp. nov.	4.42	4.42	ZD1001
Prosiphneus cf. *P. eriksoni*	4.42	4.42	ZD1001
Mimomys (*Aratomys*) *bilikeensis*	5.12	5.05	ZD0609, 0904
Apodemus sp.	5.12	5.05	ZD0609, 0904
Trischizolagus mirificus	5.12	5.05	ZD0609, 0904
Trischizolagus cf. *T. dumitrescuae*	4.42	3.26	ZD0726, 1001
Lagomorpha			
Ochotona sp. A	5.12	5.05	ZD0609, 0904
Ochotona sp. B	5.20	5.05	ZD0609, **0902**, **0904**
Ochotona sp. C	4.42	4.42	ZD1001
Ochotona sp. D	3.26	3.26	ZD0726
Carnivora			
Meles sp. n.	4.48	4.10	ZD1001, **1004**, **1208**
Panthera sp.	5.95	4.10	ZD1001, **1208**, **1223**
Vulpes sp. n.	5.08	4.42	ZD1001, 1055
Nyctereutes cf. *N. tingi*	4.10	3.97	ZD0624, 1208
Xenocyon sp.	3.81[a]	3.81[a]	ZD1205
Chasmaporthetes sp. n.	4.89	4.08	ZD**0636**, **0908**, 1029
Pliohyaena (=*Pliocrocuta*)	4.10	4.10	ZD1208
Artiodactyla			
Qurliqnoria sp.	5.29	3.31	ZD**0604**, 0745, **1202**
Bovidae genus A	4.42	4.42	ZD1001
Bovidae genus B	4.42	4.42	ZD1001
Antilospira sp.	3.62	3.62	ZD0701
Pseudois sp.	3.10	3.10	ZD0712
Metacervulus sp. n.	4.43	3.97	ZD**0624**, 1028, 1040, 1042, 1043, 1045, **1052**, 1208
Cervidae indet.	2.48	2.48	ZD0915
Palaeotragus sp.	5.30	4.57[a]	ZD1228, 1976 Xiangze Farm loc
Perissodactyla			
Hipparion zandaense	5.95	3.36	ZD0605, 0608, 0621, 0628, 0635, 0701, 0702, 0716, 0722, 0728, 0734, 0741, 0742, 0745, 0747–52, 0754, 0760, 0761, 0768, 0770, 0903, 0909, 0911–13, 0918, 0919, 1001, 1002, 1025, 1030–32, 1039, 1049, 1051, 1053, 1206, 1208, 1215, 1217, 1219, 1221, **1223**, **1232**, 1234, 1241, 1244–46
Equus sp.	2.48	0.83	ZD0915, 1220
Coelodonta thibetana	5.08	3.23	ZD0701, 0720, **0731**, 0740, 0764, 0766, 0767, 1001, 1005, 1009, 1011, 1012, **1055**, 1216, 1217, 1224, 1225, 1234, 1255, 1201, 1210
Proboscidea			
Gomphotheriidae indet.	4.44	3.81	ZD0746, 1015, 1033, **1036**, 1046, 1048, **1207**
Aves			
Struthio sp.	3.38	3.29	ZD0711, 0733
Teleosts			
Cyprinidae indet.	5.52	1.71	ZD0606, 0619, other localities not listed

[a] Indicates an estimate due to reworked status of the locality or a previous (1976) collection without precise locality information. Age resolution to less than 0.2 myr apart may not be meaningful due to systemic errors (see Section 2, Material and methods).

characteristic Pliocene mammals, particularly the small mammal assemblage from IVPP locality ZD0609 in the lower part of the section, we are able to reinterpret three previously published magnetic sections, and propose a revised correlation of the magnetic section to C1n to C3An.1r, spanning ~400 Ka to 6.4 Ma.

The lower 0–150 m is the latest Miocene part of the section. Dominated by conglomerates and other coarse-grained sediments, the lower section is sparse in fossil sites. Only five taxa are available so far: *Ochotona*, *Panthera*, *Qurliqnoria*, *Palaeotragus*, and *Hipparion*. All are consistent with a late Miocene age.

Spanning the entire Pliocene is the middle 150–620 m section. By far the most fossiliferous, this section includes a rich variety of large and small mammals. Typical for this group are such small mammals as *Nannocricetus*, *Prosiphneus*, *Mimomys*, *Apodemus*, and *Trischizolagus*, and such large mammals as *Coelodonta thibetana*, *Hipparion zandaense*, *Chasmaporthetes*, *Nyctereutes*, *Meles*, *Antilospira*, and others.

The upper 620–800 m is Pleistocene in age. This section is the least fossiliferous because of its abundant coarse gravels and conglomerates. Despite the shortage of fossil localities, we did find unambiguous Pleistocene mammals, such as *Equus*. Our lowest *Equus* locality, ZD0915, is very close to the 620 m mark, offering another excellent chronologic constraint.

Zoogeographically late Cenozoic Tibetan mammals seem to come from two major sources. A north China or east Asia component includes common elements such as *Mimomys*, *Prosiphneus*, *Trischizolagus*, *Chasmaporthetes*, *Nyctereutes*, *Meles*, and *Xenocyon*. The age relationships of these taxa outside Tibet thus offer important biochronologic constraints. The second component is the native Tibetan fauna, and this group includes pikas (*Ochotona*), squirrels (*Aepyosciurus*), and ancestral Tibetan antelope (*Qurliqnoria*). This latter assemblage does not provide age constraints by themselves, but offers important insights into indigenously evolved mammals adapted to high Tibet.

Acknowledgments

We dedicate this paper to the late Will Downs, who was passionate about biostratigraphy and dreamt of working in Zanda Basin but was robbed of that chance by cancer. We are greatly in debt to Song Yanxia and Dr. Dong Junshe, who were instrumental in securing travel and field permissions as well as various assistances for our field work in Tibet. We thank the numerous participants of our Zanda fieldwork (such as Zhao Min, Sun Boyang, Li Yangfan), whose hard work and diligent collecting have made possible our current understanding of the biostratigraphy. Field success is impossible without the dedicated services from our drivers: Shi Fuqiao, Feng Wenqing, Gao Wei, Wang Ping, and Wu Shengli, Renzeng Dawa, Tudeng Jiacuo, Ba Yixi, Ten Zeng, Ciren Laba, Ba Sang, and Lang Jie. Howell Thomas prepared some key specimens from Zanda Basin. Everett Lindsay assisted in transferring miscellaneous Zanda collections from the University of Arizona to the Natural History Museum of Los Angeles County. Wang Shifeng provided GPS coordinates for his paleomagnetic sections, and Peter Blisniuk offered useful consultation on fossil localities. The Institute of Tibetan Plateau Research, Chinese Academy of Sciences, provided room accommodations and logistic supports for field operations. Funding for fieldwork and travel are provided by the Major Basic Research Projects (2006CB806400) from the Ministry of Science and Technology of China, Strategic Priority Research Program of the Chinese Academy of Sciences (XDB03020104), CAS/SAFEA International Partnership Program for Creative Research Teams, Chinese National Natural Science Foundation (nos. 40702004 to Q.L., 40730210 to T.D., 49872011, 40128004), Chinese Academy of Science Outstanding Overseas Scholar Fund (KL205208), National Science Foundation (US) (EAR-0446699, 0444073, 0958704, 1227212 to X.W.; EAR-0958602 to Y.W.; EAR-0438115 to Peter DeCelles), and the National Geographic Society (no. W22-08 to Q.L.).

References

An, Z.-S., Kutzbach, J.E., Prell, W.L., Porter, S.C., 2001. Evolution of Asian monsoons and phased uplift of the Himalaya–Tibetan plateau since late Miocene times. Nature 311, 62–66.
Behrensmeyer, A.K., Quade, J., Cerling, T.E., Kappelman, J., Khan, I.A., Copeland, P., Roe, L., Hicks, J., Stubblefield, P., Willis, B.J., Latorre, C., 2007. The structure and rate of late Miocene expansion of C4 plants: evidence from lateral variation in stable isotopes in paleosols of the Siwalik Group, northern Pakistan. Geological Society of America Bulletin 119, 1486–1505.
Bell, C.J., Lundelius Jr., E.L., Barnosky, A.D., Graham, R.W., Lindsay, E.H., Ruez Jr., D.R., Semken Jr., H.A., Webb, S.D., Zakrzewski, R.J., Woodburne, M.O., 2004. The Blancan, Irvingtonian, and Rancholabrean mammal ages. In: Woodburne, M.O. (Ed.), Late Cretaceous and Cenozoic Mammals of North America: Biostratigraphy and Geochronology. Columbia University Press, New York, pp. 232–314.
Blois, J.L., Hadly, E.A., 2009. Mammalian response to Cenozoic climatic change. Annual Review of Earth and Planetary Sciences 37, 181–208.
Bohlin, B., 1937. Eine Tertiäre säugetier-fauna aus Tsaidam. Sino-Swedish Expedition Publication 1, 3–111.
Böhner, J., 2006. General climatic controls and topoclimatic variations in Central and High Asia. Boreas 35, 279–295.
Bolch, T., Kulkarni, A., Kääb, A., Huggel, C., Paul, F., Cogley, J.G., Frey, H., Kargel, J.S., Fujita, K., Scheel, M., Bajracharya, S., Stoffel, M., 2012. The state and fate of Himalayan glaciers. Science 336, 310–314.
Boos, W.R., Kuang, Z., 2010. Dominant control of the South Asian monsoon by orographic insulation versus plateau heating. Nature 463, 218–222.
Chaline, J., Brunet-Lecomte, P., Montuire, S., Viriot, L., Courant, F., 1999. Anatomy of the arvicoline radiation (Rodentia): paleogeographical, palaeoecological history and evolutionary data. Annales Zoologici Fennici 36, 239–267.
Chang, M., Wang, X., Liu, H., Miao, D., Zhao, Q., Wu, G., Liu, J., Li, Q., Sun, Z., Wang, N., 2008. Extraordinarily thick-boned fish linked to the aridification of the Qaidam Basin (northern Tibetan Plateau). Proceedings of the National Academy of Sciences 105, 13246–13251.
Cottle, J.M., Jessup, M.J., Newell, D.L., Searle, M.P., Law, R.D., Horstwood, M.S.A., 2007. Structural insights into the early stages of exhumation along an orogen-scale detachment: the South Tibetan Detachment System, Dzakaa Chu section, Eastern Himalaya. Journal of Structural Geology 29, 1781–1797.
Deng, T., Wang, X., Fortelius, M., Li, Q., Wang, Y., Tseng, Z.J., Takeuchi, G.T., Saylor, J.E., Säilä, L.K., Xie, G., 2011. Out of Tibet: Pliocene woolly rhino suggests high-plateau origin of Ice Age megaherbivores. Science 333, 1285–1288.
Deng, T., Li, Q., Tseng, Z.J., Takeuchi, G.T., Wang, Y., Xie, G., Wang, S., Hou, S., Wang, X., 2012. Locomotive implication of a Pliocene three-toed horse skeleton from Tibet and its paleo-altimetry significance. Proceedings of the National Academy of Sciences 109, 7374–7378.
Fejfar, O., Heinrich, W.-D., Pevzner, M.A., Vangengeim, E.A., 1997. Late Cenozoic sequences of mammalian sites in Eurasia: an updated correlation. Palaeogeography, Palaeoclimatology, Palaeoecology 133, 259–288.
Fernández, M.H., Vrba, E.S., 2005. A complete estimate of the phylogenetic relationships in Ruminantia: a dated species-level supertree of the extant ruminants. Biological Reviews 80, 269–302.
France-Lanord, C., Derry, L., 1994. Delta-C-13 of organic carbon in the Bengal Fan — source evolution and transport of C3 and C4 plant carbon to marine sediments. Geochimica et Cosmochimica Acta 58, 4809–4814.
Ganser, A., 1964. Geology of the Himalayas. Wiley InterScience, London.
Garzione, C.N., Dettman, D.L., Quade, J., DeCelles, P.G., Butler, R.F., 2000. High times on the Tibetan Plateau: Paleoelevation of the Thakkhola graben, Nepal. Geology 28, 339–342.
Gentry, A.W., 1968. The extinct bovid genus *Qurliqnoria* Bohlin. Journal of Mammalogy 49, 769.
Hodges, K.V., 2000. Tectonics of the Himalaya and southern Tibet from two perspectives. Geological Society of America Bulletin 112, 324–350.
Hodges, K.V., Parrish, R.R., Housh, T.B., Lux, D.R., Burchfiel, B.C., Royden, L.H., Chen, Z., 1992. Simultaneous Miocene extension and shortening in the Himalayan orogen. Science 258, 1466–1470.
Hodges, K.V., Parrish, R.R., Searle, M.P., 1996. Tectonic evolution of the central Annapurna Range, Nepalese Himalayas. Tectonics 15, 1264–1291.
Huang, W.-B., Ji, H.-X., 1981. The climate and uplift of the Qinghai–Xizang (Tibet) Plateau in the late Pleistocene and Holocene. In: Liu, D.-S. (Ed.), Geological and Ecological Studies of Qinghai–Xizang Plateau. Geology, Geological History and Origin of Qinghai–Xizang Plateau, vol. 1. Science Press, Beijing, pp. 225–230.
Huang, W.-B., Ji, H.-X., Chen, W.-Y., Hsu, C.-Q., Zheng, S.-H., 1980. Pliocene stratum of Guizhong and Bulong Basin, Xizang. In: Qinghai–Tibetan Plateau Comprehensive Scientific Investigation Team of Chinese Academy of Sciences (Ed.), Paleontology of Tibet, Part 1. Science Press, Beijing, pp. 4–17.
Ji, H.-X., Hsu, C.-Q., Huang, W.-B., 1980. The *Hipparion* fauna from Guizhong Basin, Xizang. In: Qinghai–Tibetan Plateau Comprehensive Scientific Investigation Team of Chinese Academy of Sciences (Ed.), Paleontology of Tibet, Part 1. Science Press, Beijing, pp. 18–32.
Kempf, O., Blisniuk, P.M., Wang, S., Fang, X., Wrozyna, C., Schwalb, A., 2009. Sedimentology, sedimentary petrology, and paleoecology of the monsoon-driven, fluvio-lacustrine Zhada Basin, SW-Tibet. Sedimentary Geology 222, 27–41.
Li, Y.Z., 2006. Xizang Annual. Xizang People Press, Lhasa.
Li, F.-L., Li, D.-L., 1990. Latest Miocene *Hipparion* (*Plesiohipparion*) of Zanda Basin. In: Yang, Z., Nie, Z. (Eds.), Paleontology of the Ngari Area, Tibet (Xi Zang). China University of Geological Science Press, Wuhan, pp. 186–193.
Lindsay, E.H., Opdyke, N.D., Johnson, N.M., 1980. Pliocene dispersal of the horse *Equus* and late Cenozoic mammalian dispersal events. Nature 287, 135–138.
Lindsay, E.H., Mou, Y.U.N., Downs, W., Pederson, J., Kelly, T.S., Henry, C., Trexler, J.I.M., 2002. Recognition of the Hemphillian/Blancan boundary in Nevada. Journal of Vertebrate Paleontology 22, 429–442.
Lourens, L., Hilgren, F., Shackleton, N.J., Laskar, J., Wilson, J., 2004. The Neogene Period. In: Gradstein, F.M., Ogg, J.G., Smith, A.G. (Eds.), A Geologic Time Scale 2004. Cambridge University Press, Cambridge, pp. 409–440.
Mascarelli, A.L., 2009. Quaternary geologists win timescale vote. Nature 459, 624.
Meng, X., Zhu, D., Shao, Z., Yang, C., Sun, L., Wang, J., Han, T., Du, J.-J., Han, J.-E., Yu, J., 2004. Discovery of rhinoceros fossils in the Pliocene in the Zanda Basin, Ngari, Tibet. Geological Bulletin of China 23, 609–612.
Meng, X., Zhu, D., Shao, Z., Yang, C., Han, J.-E., Yu, J., Meng, Q., 2005. Discovery of fossil teeth of Pliocene *Ochotona* in the Zanda Basin, Ngari, Tibet, China. Geological Bulletin of China 24, 1175–1178.
Molnar, P., 2005. Mio-Pliocene growth of the Tibetan Plateau and evolution of East Asian climate. Palaeontologia Electronica 8, 1–23.
Murphy, M.A., Harrison, T.M., 1999. Relationship between leucogranites and the Qomolangma detachment in the Rongbuk Valley, south Tibet. Geology 27, 831–834.
Murphy, M.A., Yin, A., 2003. Structural evolution and sequence of thrusting in the Tethyan fold-thrust belt and Indus–Yalu suture zone, southwest Tibet. Geological Society of America Bulletin 115, 21–34.
Murphy, M.A., Yin, A., Kapp, P.A., Harrison, T.M., Manning, C.E., Ryerson, F.J., Ding, L., Guo, J.-H., 2002. Structural evolution of the Gurla Mandhata detachment system, southwest Tibet: implications for the eastward extent of the Karakoram fault system. Geological Society of America Bulletin 114, 428–447.
National Climatic Data Center, 2012. NNDC Climate Data Online. http://www.ncdc.noaa.gov/.
Ojha, T.P., Butler, R.E., Quade, J., DeCelles, P.G., Richards, D., Upreti, B.N., 2000. Magnetic polarity stratigraphy of the Neogene Siwalik Group at Khutia Khola, far western Nepal. Geological Society of America Bulletin 112, 424–434.
Ojha, T.P., Butler, R.F., DeCelles, P.G., Quade, J., 2009. Magnetic polarity stratigraphy of the Neogene foreland basin deposits of Nepal. Basin Research 21, 61–90.
Qian, F., 1999. Study on magnetostratigraphy in Qinghai–Tibetan plateau in late Cenozoic. Journal of Geomechanics 5, 22–34.
Qiu, Z.-X., 1987. Die hyaeniden aus dem Ruscinium und Villfranchium Chinas. Münchner Geowissenschaftliche Abhandlungen 9, 1–108.
Qiu, Z.-X., 2006. Quaternary environmental changes and evolution of large mammals in North China. Vertebrata PalAsiatica 44, 109–132.
Qiu, Z.-D., Storch, G., 2000. The early Pliocene micromammalian fauna of Bilike, Inner Mongolia, China (Mammalia: Lipotyphla, Chiroptera, Rodentia, Lagomorpha). Senckenbergiana Lethaea 80, 173–229.
Qiu, Z.-X., Tedford, R.H., 1990. A Pliocene species of *Vulpes* from Yushe, Shanxi. Vertebrata PalAsiatica 28, 245–258.
Qiu, Z.-D., Wang, X., 1999. Small mammal faunas and their ages in Miocene of central Nei Mongol (Inner Mongolia). Vertebrata PalAsiatica 37, 120–139.

Qiu, Z.-X., Deng, T., Wang, B.Y., 2004. Early Pleistocene mammalian fauna from Longdan, Dongxiang, Gansu, China. Palaeontologia Sinica, New series C 27, 1–198.

Qiu, Z.-D., Wang, X., Li, Q., 2006. Faunal succession and biochronology of the Miocene through Pliocene in Nei Mongol (Inner Mongolia). Vertebrata PalAsiatica 44, 164–181.

Qiu, Z.-D., Wang, X.-M., Li, Q., in press-a. Neogene faunal succession and biochronology of central Nei Mongol (Inner Mongolia), in: Wang, X., Flynn, L.J., Fortelius, M. (Eds.), Fossil Mammals of Asia: Neogene Biostratigraphy and Chronology. Columbia University Press, New York.

Qiu, Z.-X., Qiu, Z.-D., Deng, T., Li, C.-K., Zhang, Z.-Q., Wang, B.-Y., Wang, X., in press-b. Neogene land mammal stages/ages of China — toward the goal to establish an Asian land mammal stage/age scheme, in: Wang, X., Flynn, L.J., Fortelius, M. (Eds.), Fossil Mammals of Asia: Neogene Biostratigraphy and Chronology. Columbia University Press, New York.

Quade, J., Cerling, T.E., 1995. Expansion of C4 grasses in the late Miocene of northern Pakistan: evidence from stable isotopes in paleosols. Palaeogeography, Palaeoclimatology, Palaeoecology 115, 91–116.

Quade, J., Cerling, T.E., Bowman, J.R., 1989. Development of Asian monsoon revealed by marked ecological shift during latest Miocene in northern Pakistan. Nature 342, 163–166.

Quade, J., Cater, J.M.L., Ojha, T.P., Adam, J., Harrison, T.M., 1995. Late Miocene environmental change in Nepal and the northern Indian subcontinent: stable isotopic evidence from paleosols. Geological Society of America Bulletin 107, 1381–1397.

Quade, J., Breecker, D.O., Daëron, M., Eiler, J., 2011. The paleoaltimetry of Tibet: an isotopic perspective. American Journal of Science 311, 77–115.

Repenning, C.A., 1987. Biochronology of the microtine rodents of the United States. In: Woodburne, M.O. (Ed.), Cenozoic Mammals of North America, Geochronology and Biostratigraphy. University California Press, Berkeley, pp. 236–268.

Repenning, C.A., 2003. *Mimomys* in North America. In: Flynn, L.J. (Ed.), Vertebrate Fossils and Their Context, Contributions in Honor of Richard H. Tedford, pp. 469–512.

Saylor, J., 2007. Origin of the Zhada Basin, SW Tibet: a tectonically dammed paleo-river valley. Geological Society of America Abstracts with Programs 39, 437.

Saylor, J.E., 2008. The Late Miocene Through Modern Evolution of the Zhada Basin, South-western Tibet, Department of Geosciences. University of Arizona, Tucson, p. 306.

Saylor, J.E., DeCelles, P.G., Gehrels, G.E., 2007a. Origin of the Zhada Basin, SW Tibet: a tectonically dammed paleo-river valley. Geological Society of America Abstracts with Programs 39, 437.

Saylor, J.E., DeCelles, P.G., Gehrels, G.E., Kapp, P.A., 2007b. Provenance and basin evolution, Zhada basin, southwestern Tibet. EOS. Transactions of the American Geophysical Union 88, 1340h.

Saylor, J.E., DeCelles, P.G., Quade, J., 2008. Sequence stratigraphy and frequency analysis of the Zhada Basin, SW Tibet. Eos Trans. AGU 89, Fall meeting abstract.

Saylor, J.E., Quade, J., Dettman, D.L., DeCelles, P.G., Kapp, P.A., Ding, L., 2009. The late Miocene through present paleoelevation history of southwestern Tibet. American Journal of Science 309, 1–42.

Saylor, J., DeCelles, P., Quade, J., 2010a. Climate-driven environmental change in the Zhada Basin, southwestern Tibetan Plateau. Geosphere 6, 74–92.

Saylor, J., DeCelles, P., Gehrels, G.E., Murphy, M.A., Zhang, R., Kapp, P.A., 2010b. Basin formation in the high Himalaya by arc-parallel extension and tectonic damming: Zhada Basin, southwestern Tibet. Tectonics 29, TC1004.

Searle, M.P., Parrish, R.R., Hodges, K.V., Hurford, A., Ayres, M.W., Whitehouse, M.J., 1997. Shisha Pangma Leucogranite, South Tibetan Himalaya: field relations, geochemistry, age, origin, and emplacement. Journal of Geology 105, 295–318.

Searle, M.P., Simpson, R.L., Law, R.D., Parrish, R.R., Waters, D.J., 2003. The structural geometry, metamorphic and magmatic evolution of the Everest massif, High Himalaya of Nepal–South Tibet. Journal of the Geological Society 160, 345–366.

Tedford, R.H., Qiu, Z.-X., 1991. Pliocene *Nyctereutes* (Carnivora: Canidae) from Yushe, Shanxi, with comments on Chinese fossil raccoon-dogs. Vertebrata PalAsiatica 29, 176–189.

Tedford, R.H., Wang, X., Taylor, B.E., 2009. Phylogenetic systematics of the North American fossil Caninae (Carnivora: Canidae). Bulletin of the American Museum of Natural History 325, 1–218.

Thiede, R.C., Arrowsmith, J.R., Bookhagen, B., McWilliams, M., Sobel, E.R., Strecker, M.R., 2006. Dome formation and extension in the Tethyan Himalaya, Leo Pargil, northwest India. Geological Society of America Bulletin 118, 635–650.

Tian, L., Yao, T., MacClune, K., White, J.W.C., Schilla, A., Vaughn, B., Vachon, R., Ichiyanagi, K., 2007. Stable isotopic variations in west China: a consideration of moisture sources. Journal of Geophysical Research 112, D10112.

Uyeda, J.C., Hansen, T.F., Arnold, S.J., Pienaar, J., 2011. The million-year wait for macroevolutionary bursts. Proceedings of the National Academy of Sciences 108, 15908–15913.

Wang, N., Chang, M.-M., 2010. Pliocene cyprinids (Cypriniformes, Teleostei) from Kunlun Pass Basin, northeastern Tibetan Plateau and their bearings on development of water system and uplift of the area. Science China Earth Sciences 53, 485–500.

Wang, N., Chang, M.-M., 2012. Discovery of fossil Nemacheilids (Cypriniformes, Teleostei, Pisces) from the Tibetan Plateau, China. Science China Earth Sciences 55, 714–727.

Wang, X., Qiu, Z.-D., Li, Q., Wang, B.-Y., Qiu, Z.-X., Downs, W.R., Xie, G.-P., Xie, J.-Y., Deng, T., Takeuchi, G.T., Tseng, Z.J., Chang, M.-M., Liu, J., Wang, Y., Biasatti, D., Sun, Z., Fang, X., Meng, Q., 2007. Vertebrate paleontology, biostratigraphy, geochronology, and paleoenvironment of Qaidam Basin in northern Tibetan Plateau. Palaeogeography, Palaeoclimatology, Palaeoecology 254, 363–385.

Wang, S., Blisniuk, P., Kempf, O., Fang, X., Chun, F., Wang, E., 2008a. The basin-range system along the south segment of the Karakorum Fault zone, Tibet. International Geology Review 50, 121–134.

Wang, S., Zhang, W., Fang, X., Dai, S., Kempf, O., 2008b. Magnetostratigraphy of the Zanda Basin in southwest Tibet Plateau and its tectonic implications. Chinese Science Bulletin 53, 1393–1400.

Wang, X., Xie, G.-P., Li, Q., Qiu, Z.-D., Tseng, Z.J., Takeuchi, G.T., Wang, B.-Y., Fortelius, M., Rosenström-Fortelius, A., Wahlquist, H., Downs, W.R., Zhang, C.-F., Wang, Y., 2011a. Early explorations of Qaidam Basin (Tibetan Plateau) by Birger Bohlin — reconciling classic vertebrate fossil localities with modern biostratigraphy. Vertebrata PalAsiatica 49, 285–310.

Wang, Y., Xu, Y., Khawaja, S., Wang, X., Passey, B.H., Zhang, C., Li, Q., Tseng, Z.J., Takeuchi, G.T., Deng, T., Xie, G., 2011b. Diet and environment of a mid-Pliocene fauna in the Zanda Basin (western Himalaya): paleo-elevation implications. American Geophysical Union Joint Assembly Abstract, Session T13F. Tectonics, Erosion, and Paleoclimate: Insights from Geochemistry, Paleobiology, Geochronology, and Modeling I Posters, T13F-2443.

Wang, Y., Khawaja, S., Wang, X., Passey, B.H., Xu, Y., Zhang, C., Li, Q., Tseng, Z.J., Takeuchi, G.T., Deng, T., 2012. Isotopic evidence for late Cenozoic environmental change in SW Tibet. Geological Society of America 2012 Annual Meeting, Charlotte, Session T125, Quantitative Cenozoic Terrestrial Climate Reconstructions in the Northern Hemisphere: Evidence from Paleo-Proxies and Beyond 44, Abstract 206096.

Wang, X., Flynn, L.J., Fortelius, M., in press-a. Toward a continental Asian biostratigraphic and geochronologic framework, in: Wang, X., Flynn, L.J., Fortelius, M. (Eds.), Fossil Mammals of Asia: Neogene Biostratigraphy and Chronology. Columbia University Press, New York.

Wang, X., Li, Q., Qiu, Z.-D., Xie, G.-P., Wang, B.-Y., Qiu, Z.-X., Tseng, Z.J., Takeuchi, G.T., in press-b. Neogene mammalian biostratigraphy and geochronology of Tibetan Plateau, in: Wang, X., Flynn, L.J., Fortelius, M. (Eds.), Fossil Mammals of Asia: Neogene Biostratigraphy and Chronology. Columbia University Press, New York.

Yin, A., 2006. Cenozoic tectonic evolution of the Himalayan orogen as constrained by along-strike variation of structural geometry, exhumation history, and foreland sedimentation. Earth-Science Reviews 76, 1–131.

Yin, A., Harrison, T.M., Murphy, M.A., Grove, M., Nie, S., Ryerson, F.J., Wang, X.-F., Chen, Z.-L., 1999. Tertiary deformation history of southeastern and southwestern Tibet during the Indo-Asian collision. Geological Society of America Bulletin 111, 1644–1664.

Yue, L.-P., Deng, T., Zhang, R., Zhang, Z.-Q., Heller, F., Wang, J.-Q., Yang, L.-R., 2004. Paleomagnetic chronology and record of Himalayan movements in the Longgugou section of Gyirong-Oma Basin in Xizang (Tibet). Chinese Journal of Geophysics 47, 1135–1142.

Zhang, Q.-S., Wang, F.-B., Ji, H.-X., Huang, W.-B., 1981. Pliocene stratigraphy of Zhada Basin, Tibet. Journal of Stratigraphy 5, 216–220.

Zhu, D., Meng, X., Shao, Z., Yang, C., Han, J.-E., Yu, J., Meng, Q., Lu, R., 2005. Redefinition and redivision of the Pliocene–early Pleistocene lacustrine strata in Zanda Basin, Ngari, Tibet, China. Geological Bulletin of China 24, 1111–1120.